Late Neogene evolution of modern deep-dwelling plankton

Flavia Boscolo-Galazzo[1‡*], Amy Jones[2], Tom Dunkley Jones[2], Katherine A. Crichton[1↓], Bridget S. Wade[3], Paul N. Pearson[1]

[1]Cardiff University, School of Earth and Environmental Sciences, Cardiff (UK).

[2]Birmingham University, School of Geography, Earth and Environmental Sciences, Birmingham (UK).

[3]University College London, Department of Earth Sciences, London (UK).

‡Now at Bergen University, Department of Earth Science and Bjerknes Center for Climate Research, Bergen (Norway).

↓Now at Exeter University, Department of Geography, Exeter (UK)

*corresponding author: flavia.boscologalazzo@uib.no

The fossil record of marine microplankton provides insights into the evolutionary drivers which led to the origin of modern deep-water plankton, one of the largest component of ocean biomass. We use global abundance and biogeographic data combined with depth habitat reconstructions to determine the environmental mechanisms behind speciation in two groups of pelagic microfossils over the past 15 million years. We compare our microfossil datasets with water column profiles simulated in an Earth System model. We show that deep-living planktonic foraminiferal (zooplankton) and calcareous nannofossil (mixotroph phytoplankton) species were virtually absent globally during the peak of the middle Miocene warmth. Evolution of deep-dwelling planktonic foraminifera started from subpolar-midlatitude species during late Miocene cooling, via allopatry. Deep-dwelling species subsequently spread towards lower latitudes and further diversified via depth sympatry, establishing modern communities stratified hundreds of meters down the water column. Similarly, sub-euphotic zone specialist calcareous nannofossils become a major component of tropical and sub-tropical assemblages during the latest Miocene to early Pliocene. Our model simulations suggest that increased organic matter and oxygen availability for

27 planktonic foraminifera, and increased nutrients and light penetration for nannoplankton, favored

28 the evolution of new deep water niches. These conditions resulted from global cooling and the

29 associated increase in the efficiency of the biological pump over the last 15 million years.

30 **1. Introduction**

31   The biodiversity of planktonic and nektonic organisms is difficult to explain given the uniform

32 character and vastness of pelagic environments, where genetic isolation seems difficult to maintain

33 (Norris, 2000). Planktonic microorganisms with mineralized shells have often been used as a

34 model to study the mode and tempo of species origination in the open ocean, due to the abundance,

35 widespread distribution, and temporal continuity of their fossil record (e.g., Pearson et al., 1997;

36 Norris, 2000; Bown et al., 2004; Ezard et al., 2011; Norris et al., 2013). Because of the great

37 fossilization potential of their calcium carbonate tests across much of the global ocean, their

38 relatively simple and well-established taxonomy, and highly resolved biostratigraphy, planktonic

39 foraminifera and calcareous nannofossils are amongst the most thoroughly studied . Planktonic

40 foraminifera are heterotrophic zooplankton, with different species specialized to feed on different

41 types of food, from other plankton to sinking detritus. In the modern ocean, planktonic

42 foraminifera live stratified across a range of depths spanning from the surface to hundreds of

43 meters down the water column (Rebotim et al., 2017; Meilland et al., 2019). Properties such as

44 food quantity and quality, oxygen, light and pressure all change markedly across the first few

45 hundreds of meters of the ocean. Depending on such down-column variability in environmental

46 conditions, planktonic foraminifera can actively control their living depth of preference, which

47 remains relatively stable during their adult life-stage (Hull et al., 2011; Weiner et al., 2012;

48 Rebotim et al., 2017; Meilland et al., 2019; Duan et al., 2021). A key advantage of using planktonic

49 foraminifera for evolutionary studies is the ability to extract ecological information from their shell

50   chemistry. This provides invaluable information about species-specific functional ecology (e.g.,

51   feeding strategy) and habitat preferences (e.g., surface versus deep waters), which in combination

52   with biogeographic, taxonomic, biometric, and stratigraphic data have often been used to infer

53   speciation and extinction mechanisms (Norris et al., 1993; Norris et al., 1994; Pearson et al., 1997;

54   Hull and Norris, 2009; Pearson and Coxall, 2012; Woodhouse et al., 2021) and reconstruct

55   phylogenetic relationships (Aze et al., 2011).

56   Calcareous nannoplankton also have a highly resolved and continuous fossil record; they are

57   the most abundant microfossils in oceanic pelagic sediments, and similar to planktonic

58   foraminifera, their spatial distribution ranges from tropical to subpolar latitudes (Poulton et al.

59   2017). In the modern ocean they also live stratified in the water column, with species adapted to

60   euphotic waters, and species adapted to live deeper (Poulton et al., 2017). In contrast to planktonic

61   foraminifera, nannoplankton are predominantly autotrophic, performing photosynthesis in water

62   where light penetration is sufficient, although there is evidence for heterotrophy (mixotrophic

63   behavior) in some extant (Godrjian et al., 2020) and fossil (Gibbs et al., 2020) species. In euphotic

64   waters, organic matter production from nannoplankton is at the base of pelagic food chains and of

65   the functioning of the ocean biological carbon pump. Taxonomic, biometric and stratigraphic data

66   have been used to establish phylogenetic relationships between fossil nannoplankton species

67   (Young and Bown, 1997).

68   Little emphasis has been given to the long-term drivers of evolutionary patterns observed in

69   fossil plankton from species to phylum level, although more recently, a broad connection with

70   changing climate and ocean properties has been suggested (e.g., Ezard et al., 2011; Norris et al.,

71   2013; Frass et al., 2015; Henderiks et al., 2020; Lowery et al., 2020). Boscolo-Galazzo, Crichton

72   et al. (2021) showed that over the last 15 million years the remineralization of particulate organic

73 carbon (POC) in surface waters declined markedly driven by climate and ocean cooling (Kennett

74 and Von der Borch, 1985; Kennett and Exon, 2004; Cramer et al., 2011; Zhang et al., 2014; Herbert

75 et al., 2016; Sosdian et al., 2018; Super et al., 2020), increasing the efficiency of the ocean

76 biological pump in delivering organic matter at depth. Such a mechanism was key to promote the

77 evolution of life in deep waters, allowing the development of the modern twilight zone ecosystem

78 (Boscolo-Galazzo, Crichton et al., 2021). The goal of this study is to combine the fossil record of

79 two ecologically complementary calcareous microplankton groups seldom analyzed together,

80 planktonic foraminifera and nannoplankton, and together with model simulations, help disentangle

81 the evolutionary drivers of modern deep-dwelling plankton. We use the planktonic foraminiferal

82 dataset from Boscolo-Galazzo, Crichton et al. (2021) and extend our analysis to calcareous

83 nannofossils in coeval sediment samples to assess their abundance and distribution pattern. We

84 compare the results from these two groups and contrast them against time and site-specific model

85 water column profiles for POC and oxygen (O_2) obtained from the cGENIE Earth System model.

86 Further, using stable isotopes, depth habitat reconstructions, abundance and biogeography data we

87 reconstruct the speciation mechanisms which led to the evolution of modern deep-dwelling

88 planktonic foraminiferal species.

89

90 **2. Methods**

91 **2.1 Planktonic foraminifera**

92 In this study we focus on the deep-dwelling groups of macroperforate planktonic foraminifera

93 of the hirsutellids, globorotaliids, truncorotaliids and globoconellids, which in the modern ocean

94 calcify and live mostly in the twilight zone of the ocean, i.e. between 200-1000 m (Birch et al.,
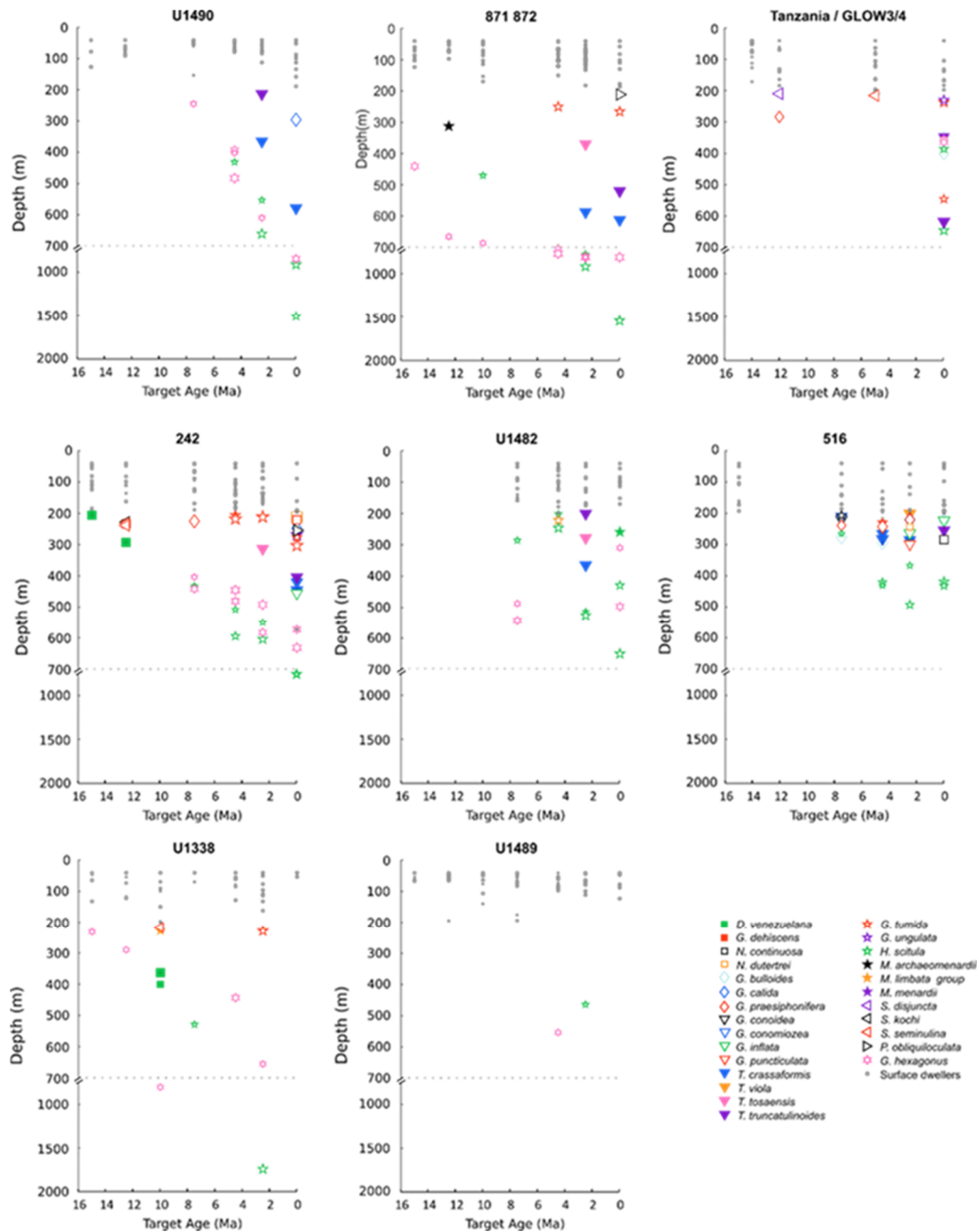
Figure 1. Depth-habitat reconstructions for middle Miocene to present planktonic foraminiferal species at the investigated sites. Surface dwellers (species living at depths shallower than 200 m) are indicated with a grey dot, deeper species are indicated with colored symbols. Relative size of symbols represents the size fractions of the sample. Reproduced from Boscolo-Galazzo, Crichton et al. (2021).

102 2012; Rebotim et al., 2017), and have a more complete fossil record than deep-dwelling

103 microperforate planktonic foraminifera (Kennett and Srinivasan, 1983).

104   Planktonic foraminiferal data and depth habitat reconstructions (Fig. 1) are from Boscolo-

105 Galazzo, Crichton et al. (2021). They were obtained from globally and latitudinally distributed

106 DSDP (Deep Sea Drilling Project)/ODP (Ocean Drilling Program)/IODP (Integrated Ocean

107 Drilling Program & International Ocean Discovery Program) sites and from cores drilled onshore

108 and offshore Tanzania, all characterized by abundant calcareous microfossils (Boscolo-Galazzo,

109 Crichton et al., 2021). The work was focused on seven target ages (15 Ma, 12.5 Ma, 10 Ma, 7.5

110 Ma, 4.5 Ma, 2.5 Ma, 0 Ma/Holocene). To avoid sample-aliasing, bulk sediment stable isotopes

111 were measured on an average of ten samples per target age at each site. The sample displaying

112 mean oxygen stable isotope values was chosen for subsequent analyses (Boscolo-Galazzo,

113 Crichton et al., 2021). Taxonomy follows: Berggren (1977), Kennett and Srinivasan (1983), Bolli

114 et al. (1989), Scott et al. (1990), Berggren (1992), Pearson (1995), Majewski (2010), Fox and

115 Wade (2013), Spezzaferri et al. (2015), Wade et al. (2018), Lam and Leckie, (2020a), with

116 phylogenetic genus names from Aze et al. (2011).

117   Ages were determined based on biostratigraphic analysis mostly following the biozonation

118 scheme by Wade et al. (2011).

119   Foraminiferal picking for stable isotope measurements were conducted from the size fractions:

120 180-250 μm, 250-300 μm, 300-355 μm (Boscolo-Galazzo, Crichton et al., 2021). Stable isotopes

121 were measured on an average of 15 different species per sample, using ~25 specimens for common

122 species, and as many specimens as possible for rare species. Stable isotopes were measured at

123 Cardiff University. Stable isotope results are shown in Fig. S1 to S9 in the Supplement. Only data

124 from the largest of the three measured size fractions are shown when data from more than one size

125 fraction are available. Data from size fractions other than those above are shown only when a

126 species did not occur within the preferred size interval. Foraminiferal abundance counts were

127 carried out in two size fractions, 180-250 μm and >250 μm, counting up to 300 specimens in each.

128 Total abundances were derived by summing up abundances from these two size fractions.

129   Boscolo-Galazzo, Crichton et al. (2021) reconstructed planktonic foraminiferal depth habitat

130 (Fig. 1) using a combined model-data approach, solving the paleotemperature equation of Kim and

131 O'Neill (1997) for each data point using measured foraminiferal δ^{18}O, global ice volume estimates,

132 and the cGENIE modeled salinity field to determine local water δ^{18}O, and then use the model

133 temperature-depth curve to determine depth. The full method is described in Boscolo-Galazzo,

134 Crichton et al. (2021).

135

136 **2.2 Calcareous Nannofossils**

137 Quantitative calcareous nannofossil data were collected from the same samples as used for

138 planktonic foraminiferal analysis or, when this was not possible, stratigraphically adjacent samples

139 (Table S1 in the Supplement). A cascading count technique was used to maximise nannofossil

140 diversity recovery and quantification of low abundance species (Styzen, 1997). Nannofossils were

141 counted per field of view (FOV) until a minimum of 400 specimens were achieved for each sample.

142 However, if a high abundance species exceeded an average of 25 specimens per FOV, it was

143 excluded from subsequent counts in that sample and its abundance scaled-up based on its average

144 abundance and the total numbers of FOV counted. Only specimens directly counted contributed

145 to the minimum count threshold of 400 specimens. An additional scan of two slide transects were

146 undertaken to record rare species not observed during the extended count and are included in the

147 total species richness and diversity analyses. Samples for nannofossil analysis were prepared using

148   the smear slide technique (Bown & Young, 1998). Calcareous nannofossils were observed using

149   both plane-polarised (PPL) and cross-polarised light (XPL) on a Zeiss Axioscope light-microscope

150   at x1000 magnification. Identification and taxonomy used herein follows Young et al. (1997) and

151   is coherent with the recent Neogene calcareous nannofossil taxonomy (Ciummelli et al., 2016;

152   Bergen et al., 2017; Blair et al., 2017; Boesiger et al., 2017; Browning et al., 2017; de Kaenel et

153   al., 2017).

154   **2.3 Plankton Ecogroups**

155   In order to compare the datasets obtained from the planktonic foraminiferal and nannofossil

156   analysis, we grouped species into ecogroups based on depth-habitat preferences. Planktonic

157   foraminiferal ecogroups are defined based on paleodepth habitat reconstructions from Boscolo-

158   Galazzo, Crichton et al. (2021): the euphotic zone ecogroups includes species with an average

159   depth habitat shallower than 200 m (the bottom of the euphotic zone), the twilight zone ecogroup

160   includes species with an average depth habitat coinciding with the twilight zone (200-1000 m).

161   The twilight zone ecogroup is largely composed of species within the globoconellids, the

162   *Globorotalia merotumida-tumida* lineage, the hirsutellids and the truncorotaliids, but also includes

163   species from other genera, such as *Globigerinella calida*, *Globorotaloides hexagonus*, *G.*

164   *variabilis*, and *Pulleniatina obliquiloculata*. *Dentoglobigerina venezuelana* has a changeable

165   depth habitat through time (Matsui et al., 2016; Wade et al., 2018); following the depth habitat

166   reconstructions from Boscolo-Galazzo, Crichton et al., (2021) it was grouped as euphotic zone

167   species for target ages 15, 12.5, 7.5, 4.5 Ma and as twilight zone species for target age 10 Ma.

168   Species were excluded from the grouping when they are known to have a marked seasonality in

169   abundance and depth habitat (*Globigerina bulloides, Globigerinella praesiphonifera* and the

170 neogloboquadrinids) (e.g., Jonkers and Kucera, 2015; Greco et al., 2019), and if they were too rare

171 and depth habitat reconstruction was not possible (*Candeina nitida*).

172 Three ecogroups for calcareous nannofossils are used: upper-euphotic, lower-euphotic and

173 sub-euphotic. The upper-euphotic group is represented by: *Discoaster* spp., *Rhabdosphaera*

174 *xiphos*, *Reticulofenestra* spp. and *Gephyrocapsa* spp. (excluding *G. ericsonii*); the lower-euphotic

175 ecogroup contains: *Rhabdosphaera clavigera, Gephyrocapsa ericsonii* and *Ceratolithus* spp.,

176 finally the subeuphotic ecogroup includes: *Florisphaera profunda* and *Calciosolena murrayi*.

177 Because species specific stable isotope measurements and depth habitat reconstructions are

178 difficult for calcareous nannofossils, species depth-habitat preference was assigned based on the

179 literature (Poulton et al., 2017; Tangunan et al., 2018). In particular, Poulton et al. (2017) described

180 vertically separated coccolithophores communities sampled during a meridional cruise in the

181 Atlantic Ocean. Here we use their criteria for assigning nannofossil species into ecogroups,

182 whereby in the upper-euphotic zone ecogroup we include species found to live in waters with

183 >10% surface irradiance, in the lower-euphotic zone ecogroup we group species found to live in

184 waters with 10-1% irradiance, and in the sub-euphotic zone ecogroup we group species found to

185 live in waters with <1%, i.e. too low to support photosynthesis (Poulton et al., 2017). *Discoaster*

186 become extinct in the early Pleistocene, therefore, its depth habitat remains under debate as the

187 group has no extant relative (Schueth and Bralower, 2015; Tangunan et al., 2018). However,

188 geochemical evidence from oxygen isotope values of *Discoaster* and planktonic foraminifera

189 (*Globorotalia menardii*, *Dentoglobigerina altispira* and *Globigerinoides obliquus*), reveal

190 comparable values and signifies that *Discoaster* likely inhabited the upper euphotic zone

191 (Minoletti et al., 2001).

192   For each target age, the relative abundance of ecogroups was calculated summing up the

193   abundance counts of all the individual species pertaining to an ecogroup at each site, hence,

194   ecogroup abundance data represent global mean values. For both nannofossils and planktonic

195   foraminifera, the percentage of each ecogroup per time bin was converted into pie-charts (Fig. 2-

196   5). Diversity indexes for both foraminiferal and nannofossil ecogroup were calculated using the

197   statistical software Past (Hammer et al., 2001) (Fig. 6).

198
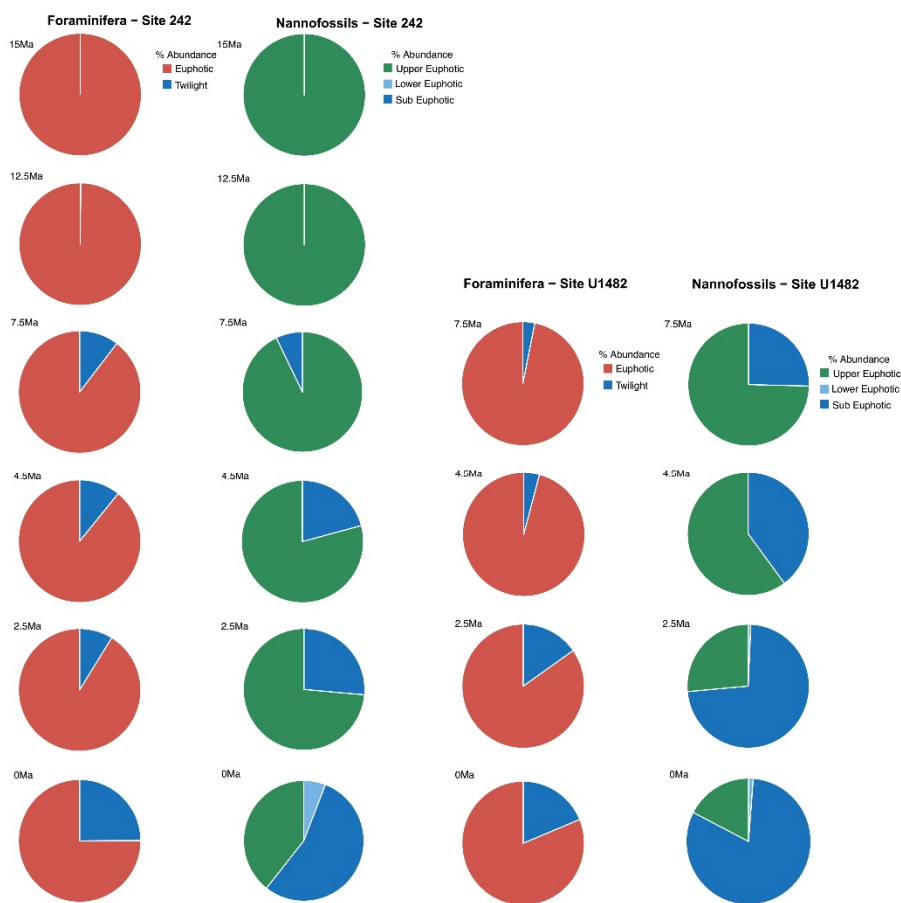
199

200   **Figure 2.** Foraminiferal and nannofossil ecogroup abundance at Site 242 and U1482.

201

202

2.4 cGENIE model

We extracted model output for Particulate Organic Carbon (POC) and oxygen concentration from the cGENIE simulations for each of the seven target ages as described fully in Boscolo-Galazzo, Crichton et al. (2021). To facilitate a general discussion of near-surface changes, we divided the data latitudinally by calculating the arithmetic mean for low latitudes (<16° latitude), two mid-latitude bands (mid 1: 16° to 40°, mid 2: 40° to 56°) and high latitudes (>56°). The cGENIE simulations take account of changing boundary conditions including CO_2 forcing, bathymetry and ocean circulation (Crichton et al., 2020). The model's ocean biological carbon pump is temperature dependent, where temperature affects both nutrient uptake rates at the surface and remineralization rates of sinking particulate organic matter down the water column (Crichton et al., 2021).

3. Results

3.1 Plankton Ecogroups

For both calcareous nannoplankton and planktonic foraminifera, the variation in abundance of euphotic zone and deeper-dwelling ecogroups show global patterns recognised across sites. Additionally both group indicate a long-term directionality towards increased abundance of deep-dwelling ecotypes. Among planktonic foraminifera, the twilight zone ecogroup increases in abundance through time starting at 7.5 Ma (Fig. 6). The relative abundance of the twilight zone ecogroup in the middle Miocene is 15% and it increases to ~30% in the Holocene time slice (Fig. 6). The average abundance of the euphotic zone species ecogroup in the middle Miocene is 85% and it decreases through time until reaching 60% in the Holocene (Fig. 6). In the twilight zone ecogroup we observe an increase in the total number of species from about 1-2 species at 15 Ma, to 14 species in the Holocene (Fig. 6). In the middle Miocene this group comprised 1/6 of the total

226   number of species in our samples, while in the Holocene it represents almost the half. All the

227   diversity indexes show a late Miocene to Holocene increasing trend for the twilight zone ecogroup

228   (Fig. 6).

229   Calcareous nannofossil assemblages are dominated by the upper-euphotic ecogroup from

230   15 to 10 Ma at all sites (Fig. 2-5). At 7.5 Ma the sub-euphotic ecogroup first becomes a significant

231   component of assemblages at Indian Ocean sub-tropical Sites U1482 and to some extent Site 242,

232   but it is not until the 4.5 Ma time slice that the sub-euphotic ecogroup becomes a significant

233   component of assemblages at the majority of locations (Sites 516, 871/872, 242, U1338, U1482,

234   U1489; Fig. 2-5). By the Holocene time slice, coccoliths of sub-euphotic species are dominant at

235   most locations, except at Eastern Equatorial Pacific Site U1338 (Fig. 6 and 4). At the southern

236   high latitude Site 1138 there is no significant contribution from coccoliths of either lower-euphotic

237   or sub-euphotic species at any point, although there is no data from the Pliocene to Holocene time

238   slices at this location (Fig. 5). Global average compositions of calcareous nannofossil assemblages

239   reflect the changes noted above, with a marked and rapid decline in the relative contribution of the

240   upper-euphotic ecogroup, and a corresponding increase in the sub-euphotic zone ecogroup through

241   the Pliocene and to Holocene (Fig. 6).

242   **3.2 Planktonic foraminiferal deep-dwelling species: depth habitat, abundance and**

243   **biogeography**

244   **3.2.1 Hirsutellids**

245   The only hirsutellid species occurring in our Miocene samples is *Hirsutella scitula*. At 15 Ma this

246   morphospecies is common only at Site 1138 (~8%), sporadically occurs at Site 516 (<1%) and is

247   absent at the other investigated sites (Fig. 7). Oxygen isotopes range from 0.5 to 1.3‰ (Fig. S1-

248

249
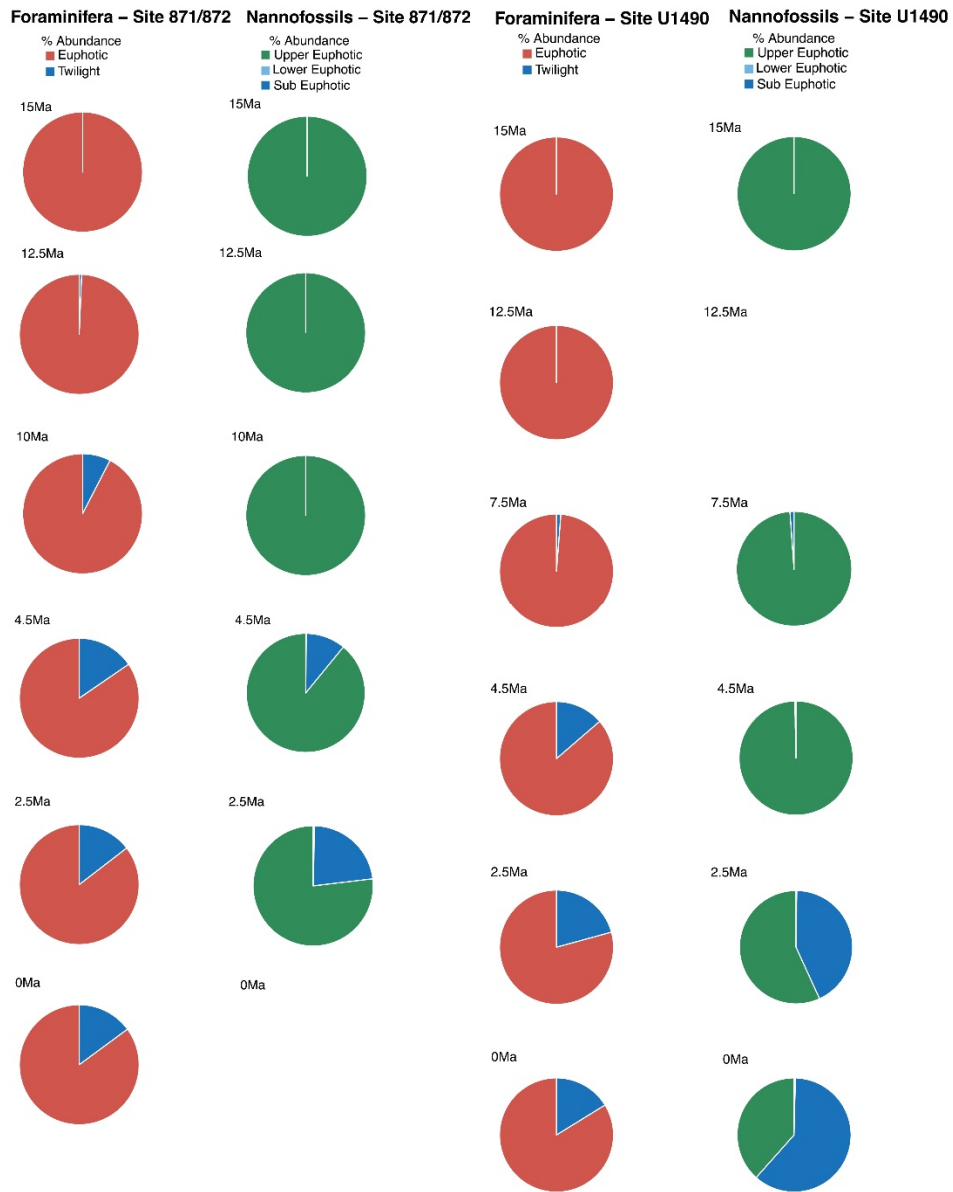
Figure 3. Foraminiferal and nannofossil ecogroup abundance at Site 871/872 and U1490.

251

252

253

254

255

256

257 S2). Depth-habitat reconstructions for Site 1138 are unattainable from δ^{18}O data due to the

258 overprinting effect of subpolar front shifts at this location, but habitat reconstruction at Site 516

259 suggests a paleodepth habitat shallower than 200 m. By 12.5 Ma, *H. scitula* appears at Site U1338

260 and U1489 in very low abundance (<0.5%) (Fig. 7). At Site U1489 the species was so rare that it

261 was encountered when picking for stable isotopes and no more when counting for species

262 abundances, despite the use of different splits of the residue. No differences were observed

263 between 12.5 and 10 Ma in the biogeography of *H. scitula* (Fig. 7). However, by 7.5 Ma, *H. scitula*

264 occurs at all our low latitude sites (Fig. 8) with oxygen isotopes ranging from -0.5 to 2.0‰ (Fig.

265 S3-S9), which according to depth habitat reconstructions translates to 250 and 500 m water depth

266 (Boscolo-Galazzo, Crichton et al., 2021). This is similar to that of *Globorotaloides hexagonus*

267 (Fig. 1)*,* the only twilight zone dweller we observed at tropical sites at 15 Ma, displaying stable

268 isotopes ranging from 0 to 1‰, which translates to depths around 300-500 m. In the late middle

269 Miocene the stable isotope values of *G. hexagonus* increase to 2-2.5‰ (Fig. S3-S9). Similarly, the

270 oxygen isotope values of tropical *H. scitula* increased through time, reaching 2-3‰ in the youngest

271 target ages. In line with this, the reconstructed depth habitat of *H. scitula* and *G. hexagonus*

272 increases through time in a stepwise fashion, and in the Holocene it reaches down to 800-1500 m

273 (Fig. 1) (Boscolo-Galazzo, Crichton et al., 2021). *Hirsutella scitula* becomes gradually more

274 common at low latitude sites through the Miocene-Pliocene, although it never becomes abundant.

275 In our record, *Hirsutella margaritae* and *H. theyeri* first appear in the early Pliocene at a depth

276 between 200-300 m (Fig. 1) (oxygen isotopes range -1 to -0.5‰), similar to that of *H. hirsuta*

277 (oxygen isotopes range 0 to 1‰) when it first appears in the Holocene (Fig. S3-S9).

278

279

280

281

282 **Figure 4.** Foraminiferal and nannofossil ecogroup abundance at Site U1338 and U1489.
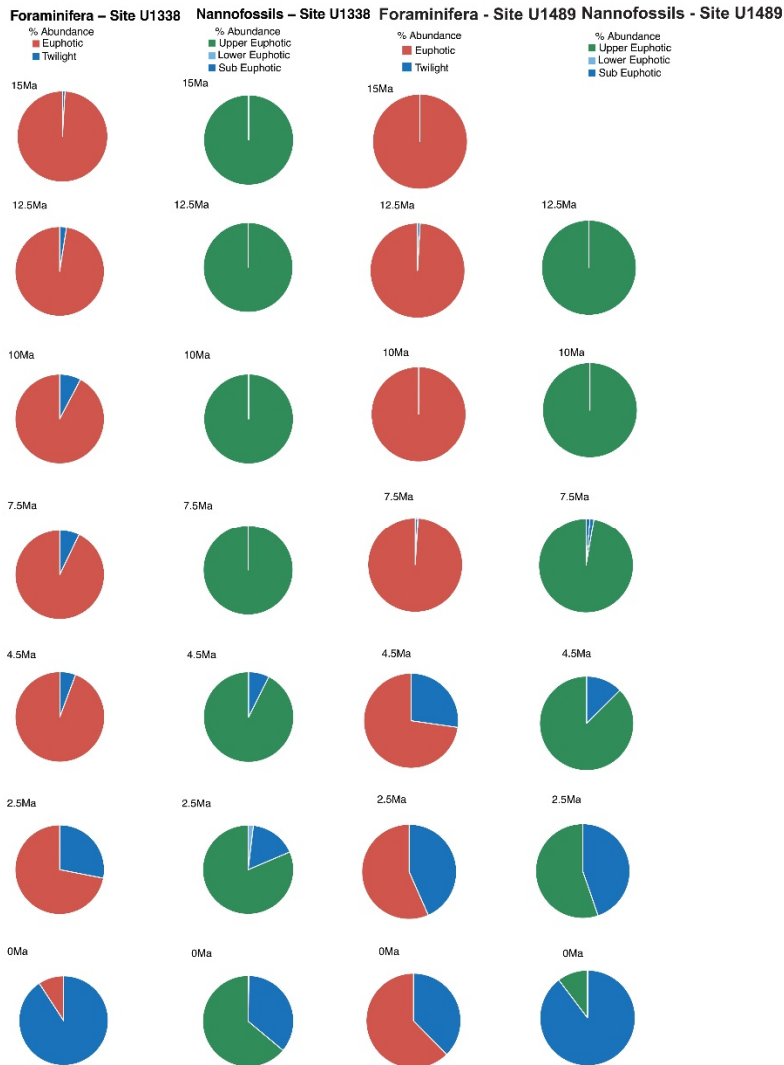
283

284

285

286

287

288

289

3.2.2 Truncorotaliids

The earliest appearances of *Truncorotalia crassaformis* in our record corresponds to our 4.5 Ma time slice at Site 1138 in the Indian Ocean sector of the Southern Ocean where it represents >20% of the assemblage, and in coeval sediments at mid-latitude Site 516 in the southwest Atlantic, where it represents ~9% of the assemblage (Fig. 9), with oxygen isotopes ranging from 1.5 to 3.0‰ (Fig. S1-S2). At Site 516 we observe the co-occurrence of *T. oceanica* (~14%) and *T. crassaformis* in the early Pliocene (4.5 Ma), and of *T. viola* (~5%) and *T. crassaformis* (~13%) in the late Pliocene (2.5 Ma) (Fig. 10). We did not observe *T. oceanica* and *T. viola* anywhere else. *T. oceanica* and *T. crassaformis* display almost overlapping $\delta^{18}O$ values and depth habitat (Fig. S2) but *T. crassaformis* has 0.5‰ lower $\delta^{13}C$ values. Oxygen stable isotope data (1‰; Fig. S2) and habitat reconstructions for Site 516 indicate that a subsurface habitat (>200 m) was already occupied by *T. crassaformis* at the beginning of its evolutionary history (Fig. 1). The late Pliocene appearance of *T. viola* at Site 516, which differs from *T. crassaformis* in having a more convex umbilical side, a triangular outline and a subacute profile, is associated with a shift to more positive oxygen isotope values of *T. crassaformis* (1.5‰) and to slightly greater depths (Fig. 1).

We find *T. crassaformis* by the late Pliocene at our investigated tropical and subtropical sites (2.5 Ma, Site U1338, U1489, 872, U1490, 242, U1482) (Fig. 10-11), with oxygen isotope values ranging from 1.0 to 2.0‰ which translate to depth habitats of 400-600 m (Boscolo-Galazzo, Crichton et al., 2021; Fig.1). The appearance of *T. crassaformis* at our low latitude sites is coeval with the appearance in our record of *Truncorotalia tosaensis*, morphologically transitional between *T. crassaformis* and *T. truncatulinoides* (Lazarus et al., 1995) (Fig. 10). *Truncorotalia tosaensis* displays oxygen isotopes values ranging from 0 to 0.5‰ (Fig. S1-S9), which translate to 300-350 m depth (Fig. 1). Consistent with earlier findings (Jenkins and Srinivasan 1986; Lam and

313 Leckie 2020b; Lazarus et al., 1995), we record the first occurrence of *T. truncatulinoides* in the

314 late Pliocene in the south-west Pacific (2.5 Ma, Site U1482), and only later in the North Pacific (0

315 Ma, Site 872), Indian Ocean (0 Ma, Site 242) and South Atlantic (0 Ma, Site 516) (Fig. 11).

316 *Truncorotalia truncatulinoides* records oxygen isotope values ranging from -1 to 2‰, more

317 negative than coeval *T. crassaformis* (Fig. S3-S9). *Truncorotalia truncatulinoides*, although

318 reported in the modern tropical ocean as one of the species living at the greatest depths, occupies

319 a shallower depth habitat than *T. crassaformis* when it first appears in our tropical to subtropical

320 records (2.5 Ma).

321

322
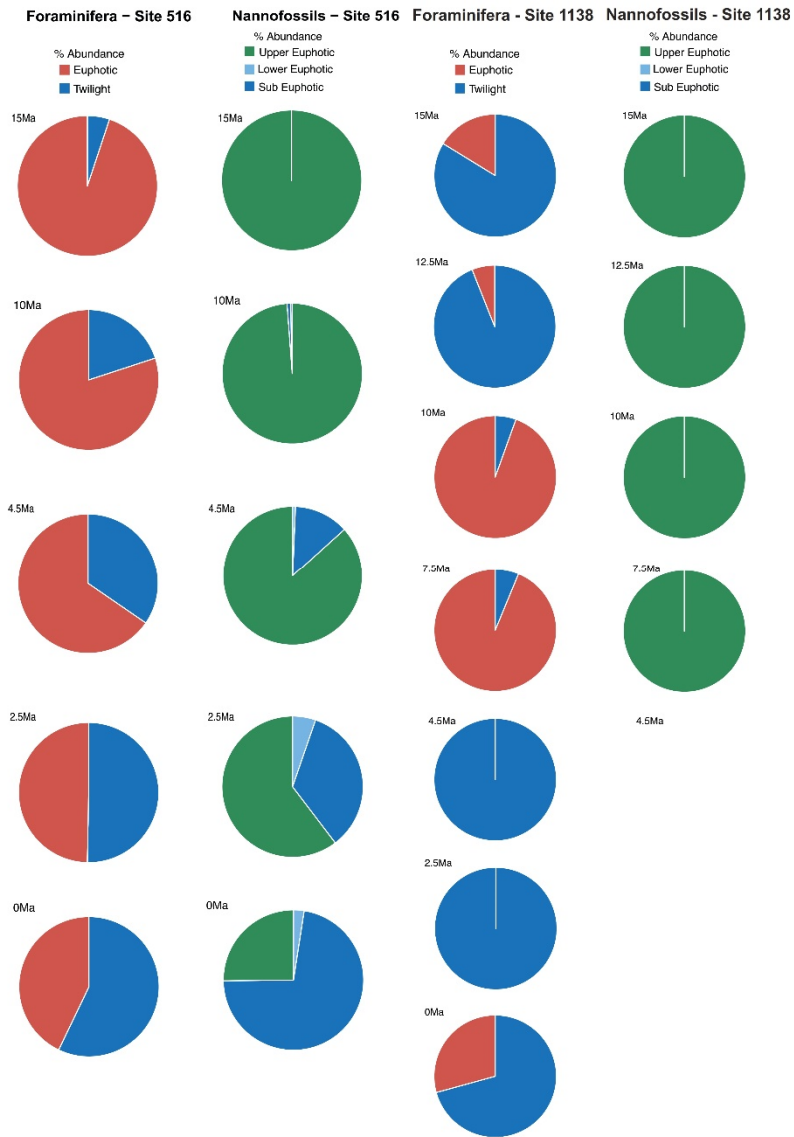
Figure 5. Foraminiferal and nannofossil ecogroup abundance at Site 516 and 1138.

323

324

325

326

327
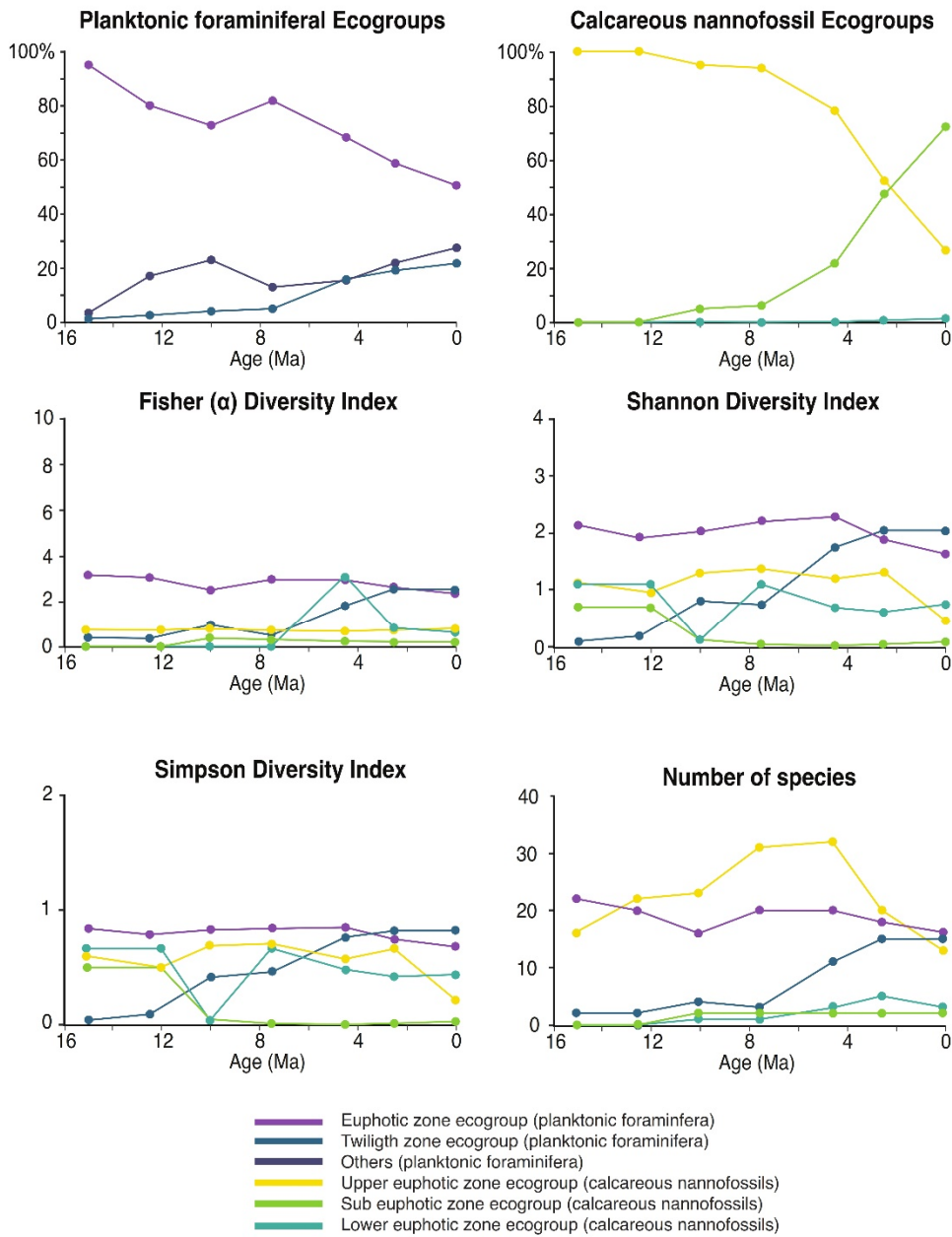
Figure 6. Planktonic foraminiferal and nannofossil ecogroups relative abundance and diversity

indexes.

330

331

332

333

3.2.3 Globorotaliids

With globorotaliids here we refer to the *Globorotalia merotumida-tumida* lineage composed by *G. merotumida*, *G. pleosiotumida*, *G. tumida* and *G. ungulata* (Kennett and Srinivasan, 1983). This group first appears with *Globorotalia plesiotumida* in our 10 Ma time slice at Site 871 (Fig. 7). At all the investigated low latitude sites, we find *G. tumida* by 4.5 Ma with abundances between 2-24% (Fig. 9). *Globorotalia plesiotumida* co-occurs with *G. tumida* only at Sites 872 and 242 corresponding to our 4.5 Ma time slice (Fig. 9; Fig. S9). In our records, *G. tumida* consistently displays oxygen isotope values between -1 to 0‰ (Fig. S3-S9), and an average depth habitat around 250 m, with a shallowest occurrence at 50 m and a deepest occurrence around 600 m (Fig. 1). Similar oxygen isotope values and depth habitat preference are recorded for *G. plesiotumida* and *G. ungulata* (Fig. 1 and Fig. S3-S9).

3.2.4 Globoconellids

In our records, *Globoconella miozea* is a dominant component of planktonic foraminiferal assemblage at Site 1138 at 15 Ma (65%) and occurs in moderate abundance at Site 516 (5%) (Fig. 7). The distribution of globoconellids appears restricted to southern high to mid-latitudes during the middle Miocene and the late Miocene to Pliocene. At Site 1138 globoconellids decrease in abundance through time, with *Globoconella panda* the only late Miocene (7.5 Ma) species (<1%; with δ^{18}O of 3‰), followed only by *Globoconella inflata* in the Holocene (4.2%; with δ^{18}O of 3.5‰) (Fig. 11). On the contrary, at Site 516 globoconellids increase in abundance through time becoming a characteristic feature of the planktonic foraminifera assemblage as noted in previous studies of this area (Berggren, 1977; Norris et al., 1994) (Fig. 7-11). In the Holocene *G. inflata* is most abundant at mid-latitude Site 516 (22.7%; with δ^{18}O of 1‰), but also occurs in the subtropical (<0.5%; with δ^{18}O of 0.9‰) and subpolar Indian ocean (4.2%; with δ^{18}O of 3.5‰) (Fig. 11; Fig.

357   S1-S3). Depth habitat reconstructions for the globoconellids show a deepening trend through time

358   although less marked compared to those of other deep-dwelling groups considered in this study

359   (Boscolo-Galazzo, Crichton et al., 2021; Fig. 1). At Site 516, the depth habitat is just above 200 m

360   for middle Miocene *Globoconella miozea* (δ^{18}O 0.9‰), just below 200 m for late Miocene *G.*

361   *miotumida* and *G. conomiozea* (δ^{18}O 1‰), and around 350 m for late Pliocene *Globoconella*

362   *puncticulata* (δ^{18}O 1.6‰) the precursor of *G. inflata,* which shows a similar depth habitat at this

363   site (δ^{18}O 1-1.2‰; Fig. S2), (Fig. 1). At Site 242 the average depth reconstruction for the Holocene

364   *G. inflata* is of ~450 m (δ^{18}O 0.9‰; Fig. S3), similar to that of *T. crassaformis* and *T.*

365   *truncatulinoides* (Boscolo-Galazzo, Crichton et al., 2021; Fig. 1).

366   **4. Discussion**

367   **4.1 Evolution of a deep-plankton ecological niche linked to late Neogene cooling**

368   We observe a trend of increasing ecological importance of deep-dwelling species in both

369   calcareous nannofossil and foraminiferal communities from the late Miocene to Recent. The

370   foraminiferal twilight zone ecogroup shows a marked increase in abundance and diversity at 7.5

371   Ma, at the same time as the first significant appearance of the sub-euphotic ecogroup within

372   coccolithophore assemblages, and coinciding with a possible acceleration of global cooling

373   (Cramer et al., 2011; Crichton et al., 2020). Fossil deep-dwelling coccoliths are dominated by one

374   species, *Florisphaera profunda,* which is often very abundant in Plio-Pleistocene sediments. This

375   makes our sub-euphotic ecogroup a low diversity – high abundance assemblage, whose origin

376   significantly impacts the relative abundance balance between ecogroups, but with little change in

377   diversity metrics towards the modern. Although there are morphological variants of *F. profunda*

378   in the modern oceans, potentially representing sub-species or pseudo-cryptic species (Quinn et al.,

379   2005), these are not distinguished in fossil assemblages and documenting their divergence times

380 requires either further molecular genetic or detailed morphological analyses. The one clear signal

381 in our diversity analyses is a late Miocene – early Pliocene peak in upper-euphotic species richness,

382 followed by a marked decline through the late Pliocene to the Holocene. The late Miocene-

383 Pliocene peak diversity is present in previous global compilations of total nannofossil diversity

384 (Bown et al. 2004; Lowery et al. 2020), but here we show that this signal is driven by first a

385 diversification and then progressive extinction almost entirely within upper-euphotic taxa.

386 Modern planktonic foraminifera evolved in two main diversification pulses in the middle Miocene

387 (16-14 Ma) and during the late Miocene-Pliocene transition (6-4.5 Ma) (Kennett and Srinivasan,

388 1983; Kucera and Schönfeld, 2007). Our species abundance and diversity data show that this

389 diversification was mostly driven by the origin of lineages of deep/subsurface dwelling species

390 (Fig. 7-11 and Fig. 6). Diversity among euphotic zone species remained constant from the middle

391 Miocene to the early Pliocene, then declined (Fig. 6). This pattern, similar to calcareous

392 nannofossils, may explain early records pointing to a decrease in Pliocene to Recent planktonic

393 foraminiferal diversity (Wei and Kennett, 1986).

394   The observed evolutionary patterns in planktonic foraminifera and coccolithophores can

395 be explained by the development of environmental conditions favourable to deep living plankton
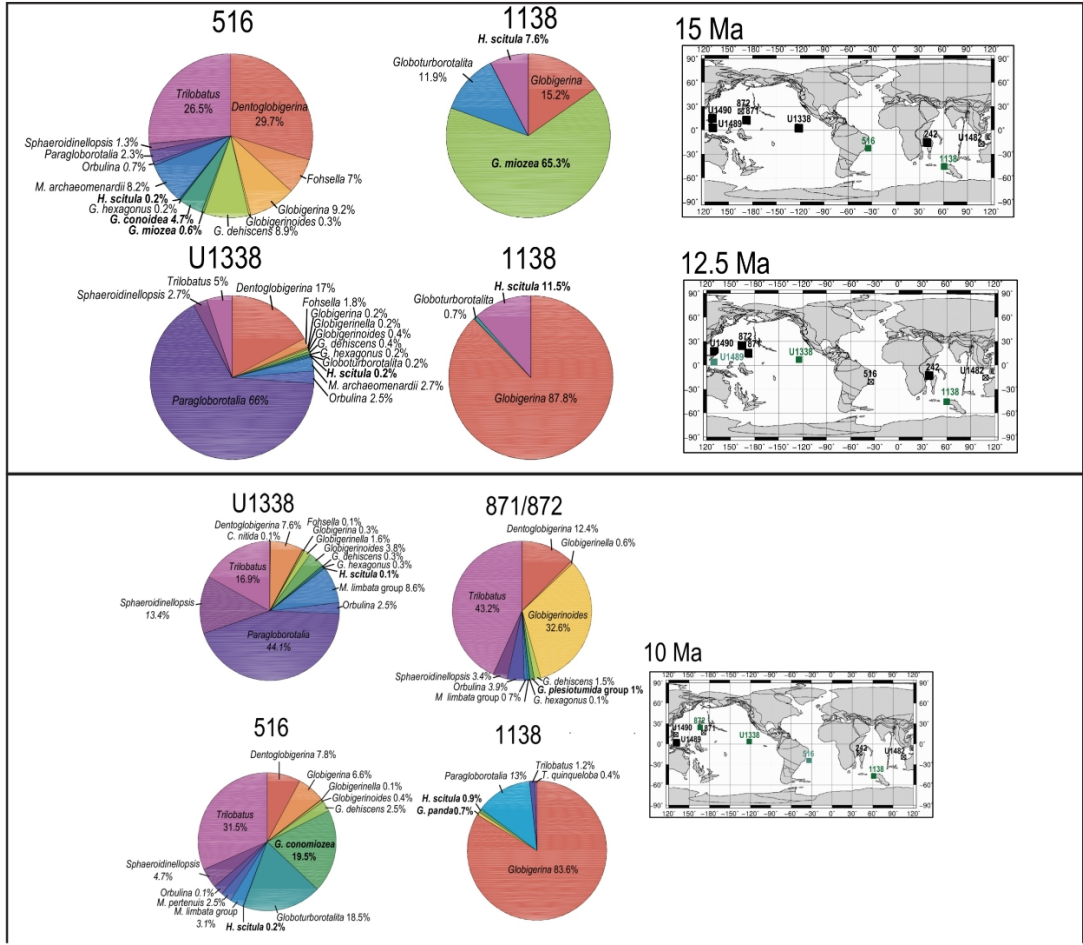
Figure 7. Abundance and biogeography of planktonic foraminiferal species at 15, 12.5, and 10 Ma. In the pie-charts twilight zone planktonic foraminiferal species are in bold. Sites where twilight zone planktonic foraminifera were found are highlighted in green in the maps. The crossed square symbol in the maps indicate that the time interval of interest was not recovered for a given site. Continental configuration follows: Ocean Drilling Stratigraphic Network (GEOMAR, Kiel, Germany).

408   with cooling. For the deep-dwelling planktonic foraminifera, survival requires the availability of

409   food at depth, and with the exception of few species adapted to oxygen minimum zones (Davis et

410   al., 2021), the absence of severe oxygen depletion. In the published literature there is a general

411   tendency for planktonic foraminiferal $\delta^{18}O$ values to be tightly grouped during times of warm

412   climate, becoming more spread-out during cooling episodes, for instance the transition from mid-

413   to late Cretaceous (Ando et al., 2010) and early to middle Eocene (John et al., 2013). In light of

414   our findings such tight $\delta^{18}O$ values, may indicate times when food and oxygen availability at depth

415   were limited, allowing planktonic foraminifera to live at shallower depths only. Because our data

416   are restricted to certain time slices and locations, we only capture a part of the overall pattern for

417   the Neogene, but other examples of depth-related evolution in the Neogene include the *Fohsella*

418   *peripheroronda – F. fohsi* lineage in the middle Miocene (Hodell and Vayavananda, 1993; Norris

419   et al., 1993) and the appearance of various deep-dwelling digitate species in the Plio-Pleistocene

420   (Coxall et al., 2007).

421   Deep-dwelling coccolithophores, most notably *Florisphaera profunda*, require dissolved

422   macronutrients (N, P) and at least some degree of light penetration (Quinn et al., 2005; Poulton et

423   al., 2017). The requirement for light penetration to depth is most clearly shown by the absence

424   of *F. profunda* beneath high surface productivity regions where nutrients are not limited at depth

425   but light is rapidly attenuated by more abundant mixed layer microplankton (Beaufort et al., 1999).

426   For coccolithophores, the cooling-driven shift from nutrient recycling within to below the mixed

427   layer, may have provided the ecological driver for species to live in deeper, more nutrient-rich

428   waters, but, as mixed layer waters cleared, also allowed the irradiance necessary for photosynthesis

429   to penetrate to these new deeper habitats. Additionally, the capability of coccolithophores to absorb

430   carbon and nutrients from seawater under low light conditions (Godrjian et al., 2020; 2021) may

431   have also aided in the occupation of new deep water niches.

432   Our model outputs from cGENIE is consistent with this interpretation, organic matter

433   export (POC at 40 m in Fig. 12) reduced with cooling, suggesting an overall decrease in primary

434   productivity at all 4 latitudinal bands considered in this study. Fewer particles in surface waters

435   would have allowed greater light penetration (Fig. 12), at the same time, the model indicates

436   enhanced organic matter delivery at >200 m with cooling. Greater organic matter delivery below

437   the euphotic zone, suggests a deeper remineralization depth and increased dissolved nutrients

438   availability at depth. This is most clearly shown in the modelled low and mid latitudes near-surface

439   waters. Oxygen availability also increased, particularly below 100 m depth in low latitudes and

440   further down the water column, below 200 m depth (Fig. 12).

441   Nonetheless, planktonic foraminifera and nannoplankton have distinct trophic statuses

442   (zoo- versus phytoplankton), further coccolithophore species require light for their dominantly

443   photosynthetic mode of life. In our data, such differences between the requirements of zoo- and

444   phytoplankton deep-dwellers is clearly observed in the biogeographic patterns. Sub-euphotic

445   coccolithophores are consistently more abundant in low nutrient sub-tropical locations (e.g. DSDP

446   Site 242 and IODP Site U1482; Fig. 2). The end-member of this biogeographic difference is ODP

447   Site 1138, in the Southern Ocean. Here, twilight foraminifera dominate most time intervals,

448   presumably due to high export production. However, lower-euphotic and sub-euphotic

449   coccolithophores are effectively excluded, due to turbid, high-productivity surface waters (Fig. 5).

450   This pattern is also supported through a comparison of high to low productivity tropical sites in

451   the Holocene – the Eastern Equatorial Pacific Site U1338 has abundant twilight foraminifera, but

452   relatively low abundances of sub-euphotic coccolithophores (Fig. 4), whereas the more

453   oligotrophic Site U1482 (Fig. 2) has lower abundances of twilight foraminifera and higher

454   abundances of sub-euphotic coccolithophores.

455   Despite these ecological differences between zoo- and phytoplankton, we suggest there is

456   a shared environmental driver for the evolution of deep-dwelling coccolithophores and planktonic

457   foraminifera linking the evolution of deep-dwelling specialists in each group. Efficient near-

458   surface recycling of organic carbon in past warm climates, such as the middle Miocene (Fig. 12),

459   precluded the occupation of the deep habitat for both groups by reducing both organic carbon

460   transfer (food limitation for foraminifera and for foraminiferal prays such copepods) and light

461   penetration (photosynthesis for coccolithophores) to depth (Fig. 2-6). Global cooling since the

462   middle Miocene (Kennett and Von der Borch, 1985; Kennett and Exon, 2004; Cramer et al., 2011;

463   Zhang et al., 2014; Herbert et al., 2016; Sosdian et al., 2018; Super et al., 2020), however, led to a

464   decreased export of organic matter and a deepening of the mean organic matter remineralization

465   depth, which in turn favoured the evolution of deep water niches in planktonic foraminifera (Fig.

466   1) and nannoplankton via increased availability of organic matter, oxygen, and likely nutrients at

467   depth (Fig. 12), and clearing of surface waters.

468

469   **4.2 Mechanisms of speciation of deep-dwelling planktonic foraminifera**

470   The hirsutellids gave rise to a large late Neogene radiation among planktonic foraminifera,

471   leading to the origin of modern phyletic groups such as the menardellids, globoconellids,

472   truncorotaliids, and the globorotaliids of the *Globorotalia merotumida - tumida* lineage (Kennett

473   and Srinivasan, 1983; Scott et al., 1986; Aze et al., 2011). The majority of the modern

474   representatives of these groups are lower euphotic zone to twilight zone species. The hirsutellids

475   originated about 18 Ma (Wade et al., 2011) from *Globorotalia zealandica* (Kennett and Srinivasan,

476   1983), the first representative of the group being *Hirsutella praescitula* (Kennett and Srinivasan,

477   1983; Aze et al., 2011). Extant hirsutellids include *H. scitula*, *H. hirsuta* and *H. theyeri*; genetic

478   data available for *H. hirsuta* indicate a single genotype (Schiebel and Hembleben, 2017). Modern

479   *H. scitula* and *H. hirsuta* are deep water forms. Depth habitat reconstructions show *H. scitula* at

480   the greatest water depth (Boscolo-Galazzo, Crichton et al., 2021; Fig. 1), consistent with it being

481   reported to have a deeper average depth habitat than *H. hirsuta* in the modern ocean (Birch et al.,

482   2013; Stainbank et al., 2019), where it feeds on suspended organic matter (Itou et al., 2001).

483   *Hirsutella hirsuta* has been reported to feed on dead diatoms and to predominantly live at depths

484   around 250 m (Schiebel and Hemleben, 2017), consistent with our habitat reconstructions placing

485   *H. hirsuta* and other hirsutellids shallower than *H. scitula*, between the bottom of the euphotic

486   zone and the upper twilight zone. Our depth habitat reconstruction for *H. scitula* at Site 516 for

487   the 15 Ma time slice, indicates an initial euphotic zone depth habitat preference for this species.

488   By the 7.5 Ma time slice, we find *H. scitula* at most of our low latitude sites, at depth comprised

489   between 300-500 m (Fig. 1). We suggest that the spread of *H. scitula* from high-mid latitudes

490   towards the tropics after the middle Miocene warmth (Fig. 7-11) tracks increasing availability of

491   POC and oxygen at depth (Boscolo-Galazzo, Crichton et al., 2021; Fig. 12), allowing this species

492   to find food in deep tropical twilight zone waters, profiting from a new ecological niche. We

493   suggest that moving from a surface to a deep-water habitat was for *H. scitula* an ecological

494   innovation which allowed the species to move outside its high-mid latitude areal, consistent with

495   observations from the modern ocean documenting *H. scitula* dwelling at progressively deeper

496   depth from high to tropical latitudes (Schiebel and Hemleben, 2017). The proceeding ocean

497   cooling (and increasing efficiency of the biological pump) explains the stepwise depth habitat

498   increase of *H. scitula* through time at tropical and subtropical sites (Fig.1): more food became

499   available at increasingly greater depth in association with improved oxygen availability (Fig. 12),

500   allowing the species to expand its habitat

501

502
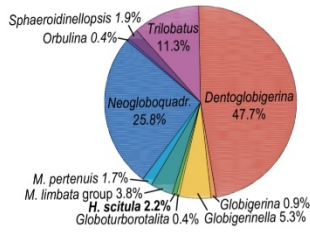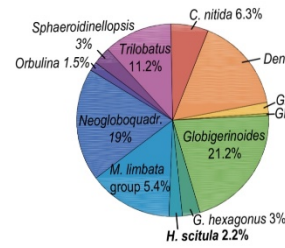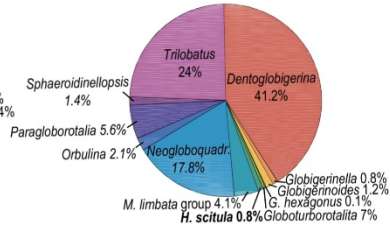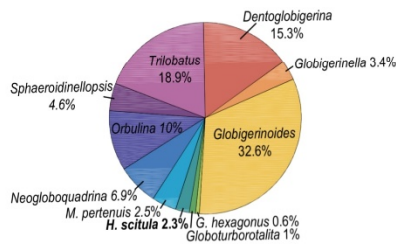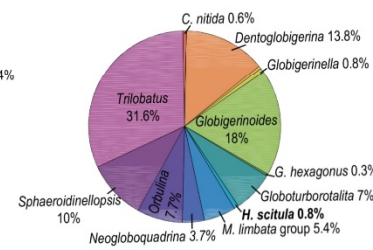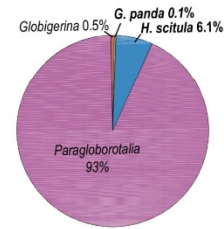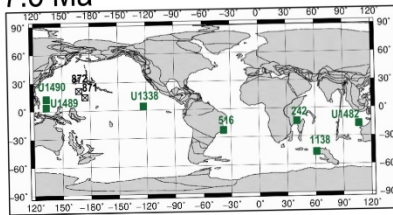
Figure 8. Abundance and biogeography of planktonic foraminiferal species at 7.5 Ma. In the pie-charts twilight zone planktonic foraminiferal species are in bold. Sites where twilight zone planktonic foraminifera were found are highlighted in green in the maps. The crossed square symbol in the maps indicate that the time interval of interest was not recovered for a given site. Continental configuration follows: Ocean Drilling Stratigraphic Network (GEOMAR, Kiel, Germany).

509

510

511

512

513

514
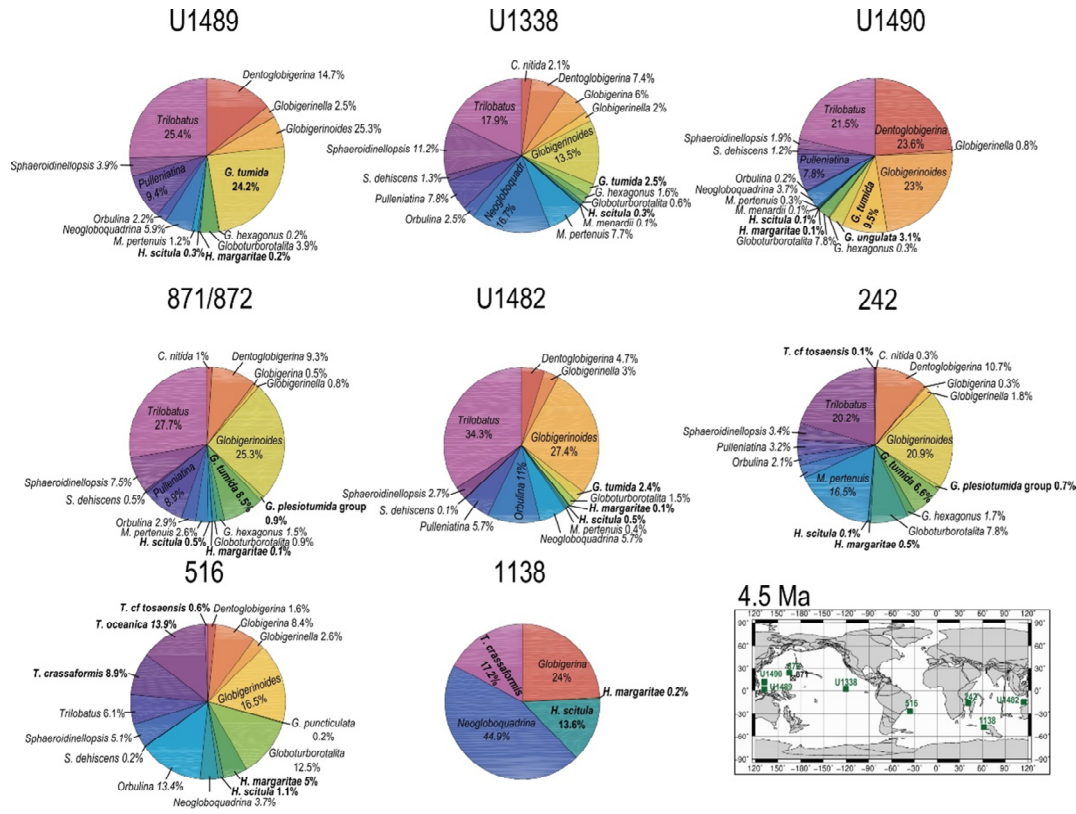
Figure 9. Abundance and biogeography of planktonic foraminiferal species at 4.5 Ma. In the pie-charts twilight zone planktonic foraminiferal species are in bold. Sites where twilight zone planktonic foraminifera were found are highlighted in green in the maps. The crossed square symbol in the maps indicate that the time interval of interest was not recovered for a given site. Continental configuration follows: Ocean Drilling Stratigraphic Network (GEOMAR, Kiel, Germany).

521

522

523

524

525   vertically other than geographically. At low latitude sites this was accompanied by speciation, with

526   the appearance of *Hirsutella margaritae* and *H. theyeri* in the early Pliocene, and of *H. hirsuta* in

527   the Holocene. These new species display depth habitats shallower than *H. scitula* at their

528   appearance. Hence, we suggest that it was the occupation of a new deep water habitat in tropical

529   waters that triggered speciation from *H. scitula* through depth sympatry, i.e. genetic isolation

530   attained in the same area but at different depths (Weiner et al., 2012). Earlier studies on speciation

531   among planktonic foraminifera based on the fossil record, highlighted a predominance of

532   sympatric speciation, possibly linked to changes in ecology (Norris et al., 1993; Lazarus et al.,

533   1995; Pearson et al., 1997). This has more recently been supported by genetic analysis, which

534   reveals a consistent depth separation between intra-specific genotypes at a global scale, suggesting

535   that depth sympatry could be a universal mechanism generating diversity among microplankton

536   (Weiner et al., 2012).

537   Truncorotaliids start their evolutionary history at ~4.31 Ma (Raffi et al., 2020), when

538   *Truncorotalia crassaformis* splits from *Hirsutella cibaoensis* (Kennett and Srinivasan, 1983; Aze

539   et al., 2011), one of the first new species originating from *H. scitula* after its spread to low latitudes

540   (Kennett and Srinivasan, 1983). Our reconstructed geographic and temporal distribution for *T.*

541   *crassaformis* suggests that the early Pliocene split from the hirsutellids happened in cold subpolar

542   water. By the early Pliocene *Truncorotalia crassaformis* was an abundant component of the

543   subpolar assemblage at Site 1138 (>17%) and had already successfully spread to middle latitudes

544   (>8%) but does not occur in our low latitude samples (Fig.9).

545
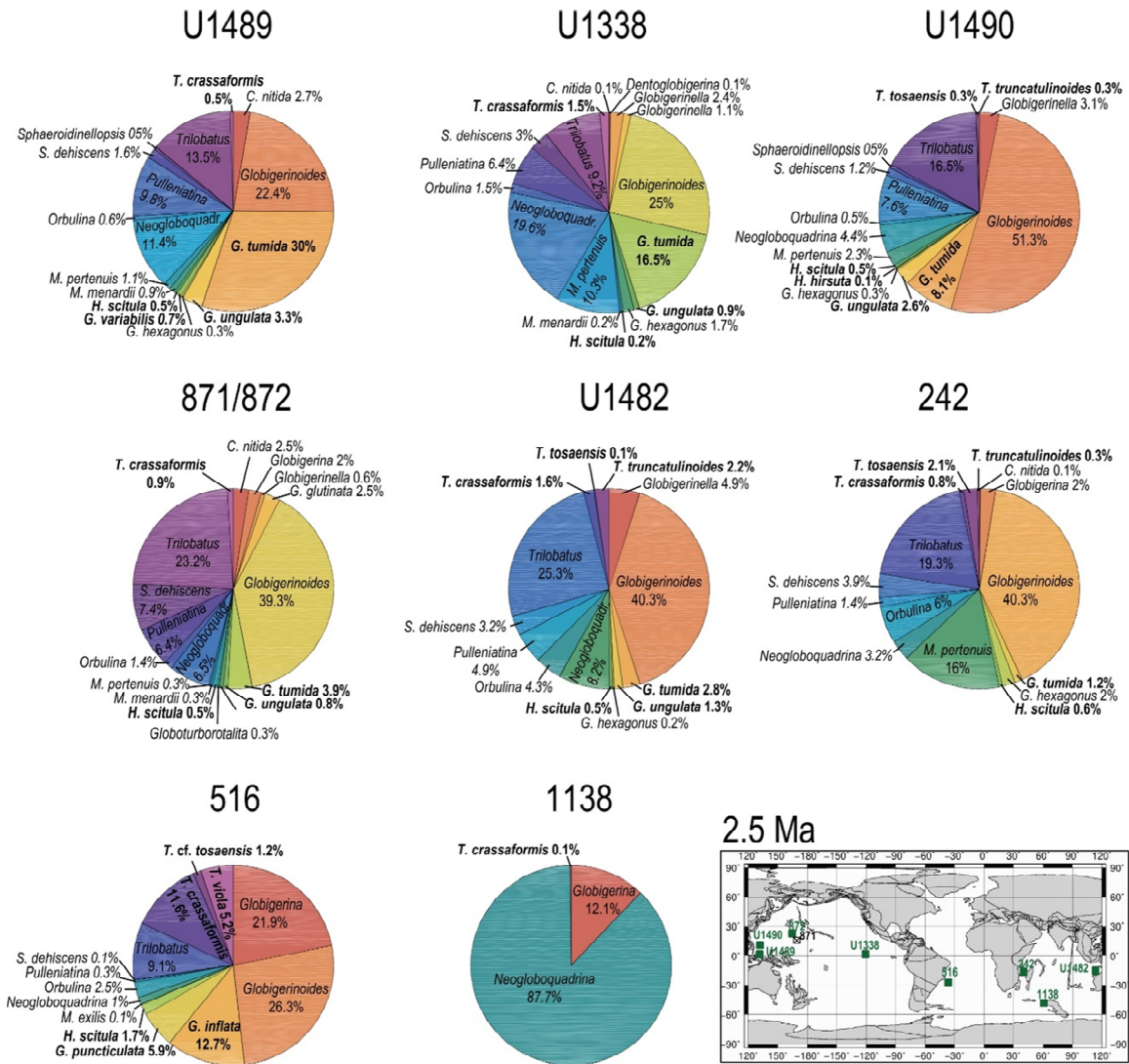
548 **Figure 10.** Abundance and biogeography of planktonic foraminiferal species at 2.5 Ma. In the pie-
549 charts twilight zone planktonic foraminiferal species are in bold. Sites where twilight zone
550 planktonic foraminifera were found are highlighted in green in the maps. The crossed square
551 symbol in the maps indicate that the time interval of interest was not recovered for a given site.
552 Continental configuration follows: Ocean Drilling Stratigraphic Network (GEOMAR, Kiel,
553 Germany).

554

555
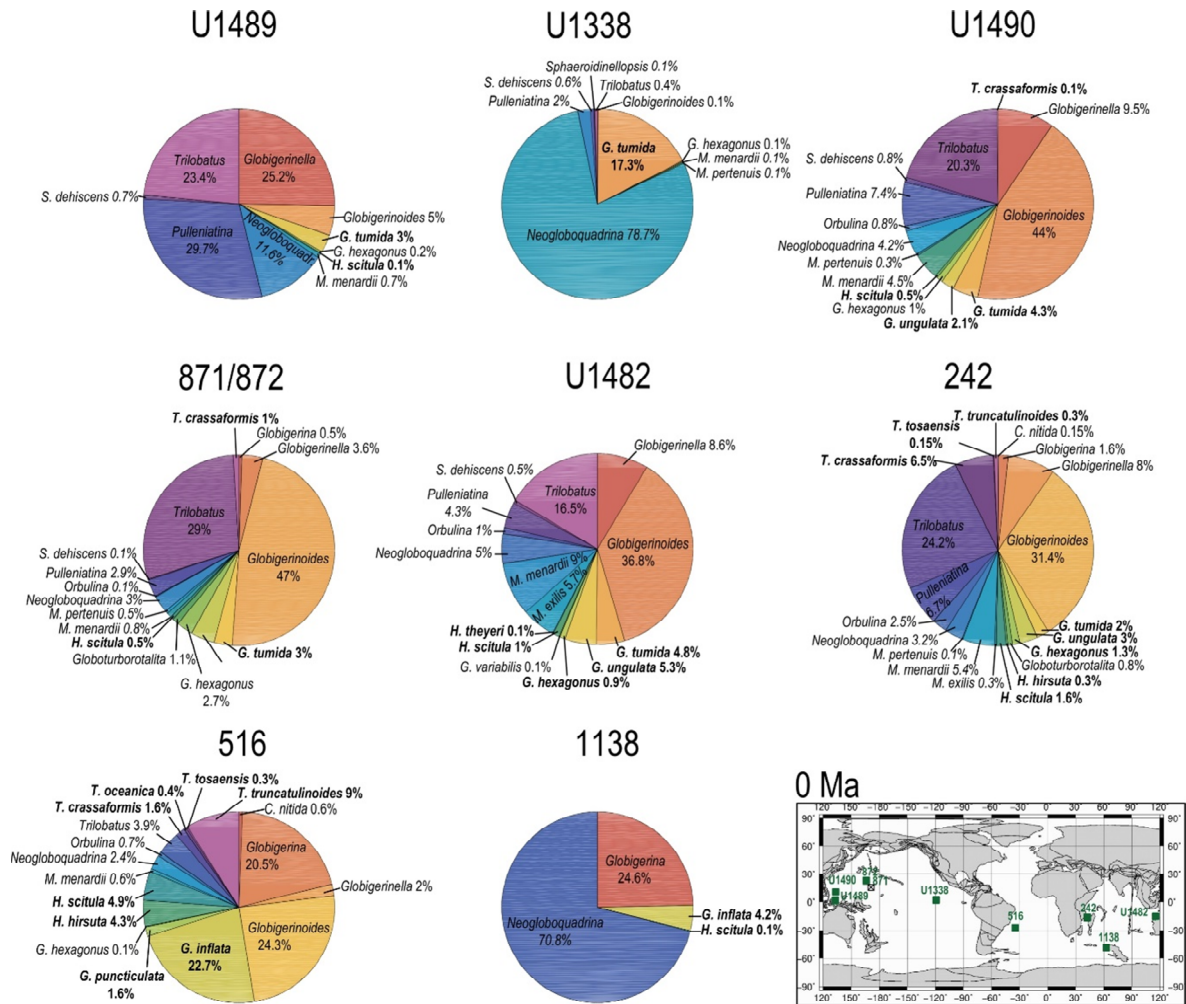
Figure 11. Abundance and biogeography of twilight zone planktonic foraminiferal species at 0

Ma. In the pie-charts twilight zone planktonic foraminiferal species are in bold. Sites where

twilight zone planktonic foraminifera were found are highlighted in green in the maps. The crossed

square symbol in the maps indicate that the time interval of interest was not recovered for a given

site. Continental configuration follows: Ocean Drilling Stratigraphic Network (GEOMAR, Kiel,

Germany).

562

563   Although modern planktonic foraminifera have a high dispersal potential (Darling et al., 2000;

564   Norris and De Vergas, 2000), our data suggest that the evolution of *Truncorotalia crassaformis*

565   from the hirsutellids might have happened through allopatry, with low latitude population of *H.*

566   *cibaoensis* becoming isolated from subpolar populations and eventually evolving into *T.*

567   *crassaformis* (e.g., following the development of diachrony reproductive seasons in high and low

568   latitude populations). Similar to *H. scitula,* from subpolar latitudes, *Truncorotalia crassaformis*

569   appears to have subsequently spread to lower latitudes occupying progressively deeper habitats

570   (Fig. 1; Fig. 7-11), and originating numerous daughter species, some of which are intermediate

571   morphospecies with limited geographic distributions no longer extant today (Lazarus et al., 1995).

572   At Site 516 we find *Truncorotalia viola*, with lighter $\delta^{18}O$ and $\delta^{13}C$ values than *T. crassaformis*

573   (Fig. S2), pointing to a clear ecological differentiation. Together with the marked morphological

574   differentiation between the two, this suggests *T. viola* may have been a different biological species.

575   *Truncorotalia truncatulinoides*, the most representative species of this group, appears to have

576   originated from *T. crassaformis* at about 2.7 Ma in the tropical southwest Pacific, and subsequently

577   spread in the global ocean (Dowsett, 1988; Lazarus et al., 1995). According to our reconstruction,

578   depth sympatry associated with gradual morphological changes characterizes speciation among

579   the truncorotaliids, as depth habitat deepening of the ancestor/precursor is clear in the transition *T.*

580   *crassaformis-T. viola* and *T. crassaformis-T. tosaensis-T. truncatulinoides* in our record (Fig. 1).

581   The possibility to colonize deeper water habitats may have led to progressive reproductive

582   isolation between "deeper" and "shallower" populations of *T. crassaformis*, resulting in biological

583   speciation. Depth sympatry as speciation mechanism for the truncorotaliids was already proposed

584   by Lazarus et al. (1995) based on biogeography, but without a definitive test.

585   In the modern ocean the *Globorotalia merotumida-tumida* lineage is represented by *G.*

586   *tumida* and *G. ungulata*, distributed in tropical to temperate regions. Genetic analysis has revealed

587   that they are two distinct biological species with a single genotype each (Schiebel and Hemleben,

588   2017). Little is known about the ecology of these two species, although *G. tumida* is known to

589   dwell in subsurface waters at the deep chlorophyll maximum (Schiebel and Hemleben, 2017).

590   According to the phylogeny of Aze et al. (2011), *Menardella menardii* gave rise to the

591   *Globorotalia merotumida-tumida* lineage around 9 Ma. However, *Menardella menardii* is absent

592   in our late Miocene samples while other menardellids such *Menardella limbata* and *M. pertenuis*

593   are common at several of our investigated middle latitudes to tropical sites. By 4.5 Ma,

594   *Globorotalia tumida* had evolved and is common at all of our low latitude sites (Fig. 9), while *M.*

595   *menardii* is extremely rare, occurring only at Sites U1338 and U1490 (0.1%), becoming more

596   common only by the Holocene. Based on this biogeographic pattern, we propose that the *G.*

597   *merotumida-tumida* lineage originated from a late Neogene menardellid, such for instance *M.*

598   *limbata* which is morphologically very similar to *G. merotumida*. Given that *G. plesiotumida* and

599   *G. tumida* display a deeper habitat (> 200 m) than *M. limbata* and other Miocene menardellids

600   (100-200 m), we suggest that such transition may have happened through depth sympatry in

601   tropical waters, with forms which remained reproductively isolated in the twilight zone generating

602   the *G. merotumida-tumida* lineage. Morphometric measurements on *M. limbata* and *G.*

603   *merotumida* shells are required to test for an evolutionary relationship between these two species.

604   According to our depth habitat reconstruction, *G. plesitumida* and *G. tumida* occupied a similar

605   depth habitat at 4.5 Ma, so it is not clear from our dataset which evolutionary mechanism may

606   have led to the origination of the latter from the first. Hull and Norris (2009) analyzed speciation

607   within this lineage and suggested that the evolution from *G. plesiotumida* to *G. tumida* happened

608   abruptly within 44 kyr. *Globorotalia ungulata*, appears in our record by the late Pliocene and often

609   display a habitat shallower than *G. tumida*, suggesting depth sympatry as the evolutionary

610   mechanism leading from *G. tumida* to *G. ungulata*. However, because depth habitat

611   reconstructions for these two species are more variable and shallower than that of other twilight

612   zone species, more data are required to more conclusively infer speciation mechanisms.

613   The globoconellids originated in the late early Miocene (~17 Ma) with *Globoconella*

614   *miozea*, which is considered to descend directly from *Hirsutella praescitula* (Kennett and

615   Srinivasan, 1983; Scott et al., 1990; Norris et al., 1994; Aze et al., 2011). *Globoconella miotumida*

616   originated in the middle Miocene and, after the extinction of *G. miozea* at about 10 Ma, remained

617   the only representative of the globoconellids until the latest Miocene. At this time, the evolutionary

618   turnover within the group accelerated and a number of different morphospecies originate from *G.*

619   *miotumida* and go extinct very rapidly, until the appearance in the late Pliocene of *G. inflata* which

620   persists until today (Wei and Kennett, 1988; Wei, 1994; Aze et al., 2011). Compared to other

621   Neogene to Recent taxa, the globoconellids display a more restricted geographic distribution

622   throughout their evolutionary history. They tend to be common at mid latitude hydrographic fronts

623   (Schneider and Kennett, 1999; Schiebel and Hemleben, 2017; Lam and Leckie, 2020; Brombacher

624   et al., 2021), except *G. puncticulata* and *G. inflata*, which extend into low latitude regions (Norris

625   et a., 1994). The geographic distribution of globoconellids as shown here suggests that this group

626   was already specialized to live at hydrographic fronts in the middle Miocene, possibly feeding on

627   phytoplankton. Starting at ~5.5 Ma, cooling and the possibility to feed on sinking detritus in deeper

628   waters (Boscolo-Galazzo, Crichton et al., 2021) may have stimulated evolutionary turnover within

629   this otherwise rather static group. The closely spaced temporal succession of morphospecies at this

630   time may reflect ongoing evolutionary experiments in an attempt to profit from new ecological

631 possibilities opening up at depth and outside the area of the group. The depth habitat

632 reconstructions for *G. puncticulata* and *G. inflata* suggests that from the Pliocene this group started

633
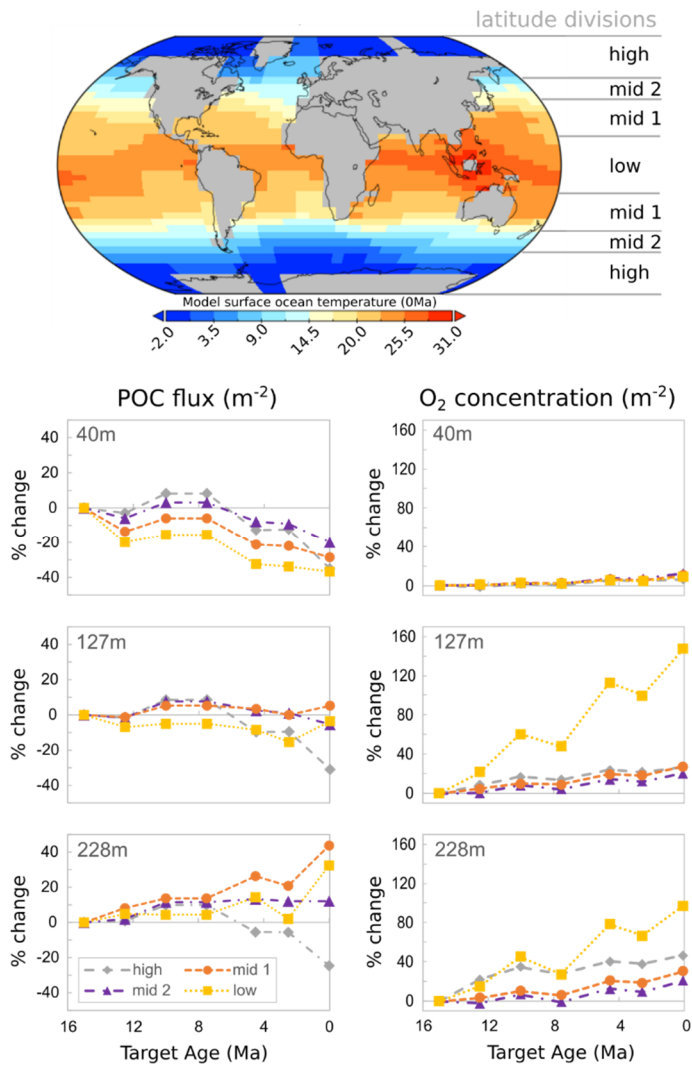
Figure 12. cGENIE model output for changes in Particulate Organic Carbon (POC) flux, and

635 dissolved Oxygen in near-surface ocean waters from the middle Miocene to Present, with a

636 temperature-dependent biological carbon pump. Inset map shows the modelled Present surface

637 ocean temperatures. Depths are the middle of cGENIE's top three ocean layers.

638

639 to progressively adapt to greater depths, consistent with the distinctive change in morphology

640 between *G. sphericomiozea* (and other Miocene globoconellids) and its Pliocene descendants *G.*

641 *puncticulata* and *G. inflata* (Kennett and Srinivasan, 1983), as well as with previous stable isotope

642 reconstructions for these species (Schneider and Kennett, 1996). We suggest that an evolutionary

643 transition began with the morphospecies *G. puncticulata*, transitional between *G. sphericomiozea*

644 and *G. inflata* and led to the late Pliocene speciation of *G. inflata*. It is not clear from our data

645 whether depth sympatry or allopatry allowed the speciation of *G. inflata,* as *G. puncticulata* and

646 *G. inflata* show similar depth habitat in our record. It may have been a combination of the two,

647 given *G. inflata* genotypes display a characteristic allopatric distribution in the ocean (Morard et

648 al., 2011).

649   Our data indicate that combining stable isotopes and model-derived water column temperature

650 is a promising approach to quantify the depth habitat of extinct planktonic foraminiferal species.

651 When combined with abundance and biogeographic data, depth habitat reconstructions offer

652 insights into speciation mechanisms not resolvable with the use of one technique alone (e.g., stable

653 isotopes). Our reconstructions indicate that both allopatry and depth sympatry played a role in the

654 origin of modern deep-dwelling planktonic foraminiferal species. Both allopatry and depth

655 sympatry appear to have been involved with the cladogenesis of the truncorotaliid and the

656 globorotaliid lineages, while depth sympatry seems to be mostly involved for intra-lineage

657 speciation.

658 **5. Conclusions**

659   Our global abundance and biogeographic data combined with our depth habitat

660 reconstructions allow us to piece together the environmental drivers behind speciation in two of

661 the most extensively studied group of pelagic microfossils, planktonic foraminifera and calcareous

662   nannofossils over the last 15 million years. The evolution of the new Neogene deep-water lineages

663   of the hirsutellids, globorotaliids, globoconellids and truncorotaliids, and of nannoplankton lower-

664   euphotic zone and sub-euphotic zone species, resulted in the vertical stratification of species seen

665   in the modern ocean, in particular at low latitudes. For planktonic foraminifera such vertical

666   stratification of species, hundreds of meters below the surface, originated through depth sympatry

667   as well as cladogenesis of new lineages via both sympatry and allopatry.

668   Our study places the evolution of modern plankton groups in the context of large scale

669   changes in ocean macroecology driven by the global climate dynamics of the past fifteen million

670   years. The late Miocene to present evolutionary history of planktonic foraminifera and

671   nannoplankton was linked, wherein increased efficiency of the biological pump with cooling since

672   the middle Miocene was a shared evolutionary driver. Lower rates of organic matter

673   remineralization in the upper part of the water column allowed the creation of new ecological

674   niches in deep waters, by increasing food delivery and oxygen at depth for heterotrophic planktonic

675   foraminifera, and by clearing surface waters and augmenting the concentration of macronutrients

676   at depth for nannoplankton.

677

678 **Data availability:** All data associated with this article are available in the Supplement or have

679 been previously published. The code is tagged as v0.9.18 and is available at DOI:

680 10.5281/zenodo.4469673 and at: DOI: 10.5281/zenodo.4469678.

681

682 **Author contributions:**

683 Conceptualization, F.B.G. and P.N.P.; investigation, F.B.G. (planktonic foraminifera) and A.J.

684 (nannofossils); software, K.A.C.; writing–original draft, F.B.G.; writing–review and editing,

685 F.B.G., A.J., T.D.J, K.A.C., P.N.P., B.S.W.; visualization, F.B.G., A.J., K.A.C.; project

686 administration and funding acquisition, P.N.P. and B.S.W.

687

688 **Competing interests:**

689 The authors declare that they have no conflict of interest.

690 **Acknowledgements:**

691 Supported by Natural Environment Research Council (NERC) grant NE/N001621/1 to P.N.P.

692 (F.B.G. and K.A.C.), NERC grant NE/P019013/1 to B.W and NERC grant NE/P016375/1 to

693 participate in IODP Expedition 363 (P.N.P.). A.J. was founded by a CENTA Doctoral Training

694 Programme as part of NERC grant: NE/L002493/1 to T.D.J. We thank Ian Hall for becoming

695 acting Principal Investigator in the later stages of the grant and Jamie Wilson for insightful

696 discussions.

697

698 **References**

699 Ando, A., Huber, B.T., and MacLeod, K.G.: Depth-habitat reorganization of planktonic

700 foraminifera across the Albian/Cenomanian boundary, Paleobiology, 36, 357-373, 2010.

701 Aze, T., Ezard, T.H.G., Purvis, A., Coxall, H.K., Stewart, D.R.M., Wade, B.S., and Pearson, P.N.:

702 A phylogeny of Cenozoic macroperforate planktonic foraminifera from fossil data, Biological

703 Reviews, 86, 900–927, 2011.

704 Bergen, J.A., de Kaenel, E., Blair, S.A., Boesiger, T.M., and Browning, E.: Oligocene-Pliocene

705 taxonomy and stratigraphy of the genus Sphenolithus in the circum North Atlantic Basin: Gulf of

706 Mexico and ODP Leg 154, J. Nannoplankt. Res. 37, 77–112, 2017.

707 Berggren, W.A.: Late Neogene planktonic foraminiferal biostratigraphy of the Rio Grande Rise

708 (SouthAtlantic). Mar. Micropaleontol., 2, 265-313, 1977.

709 Berggren, W.A.: Neogene planktonic foraminifer magnetostratigraphy of the southern Kerguelen

710 Plateau (Sites 747, 748, 751). In: Wise, SW; Schlich, R; et al. (eds.), Proceedings of the Ocean

711 Drilling Program, Scientific Results, College Station, TX (Ocean Drilling Program), 120, 631-647,

712 1992.

713 Birch, H., Coxall, H.K., Pearson, P.N., Kroon, D., and O'Regan, M.: Planktonic foraminifera

714 stable isotopes and water column structure: Disentangling ecological signals, Marine

715 Micropaleontology, 101, 127–145, 2013.

716 Blair, S.A., Bergen, J.A., de Kaenel, E., Browning, E., and Boesiger, T.M.: Upper Miocene-Lower

717 Pliocene taxonomy and stratigraphy in the circum North Atlantic Basin: radiation and extinction

718 of Amauroliths, Ceratoliths and the D. quinqueramus lineage, Journal of Nannoplankton Research.

719 37, 113–144, 2017

720   Boesiger, T.M., de Kaenel, E., Bergen, J.A., Browning, E., and Blair, S.A.: Oligocene to

721   Pleistocene taxonomy and stratigraphy of the genus Helicosphaera and other placolith taxa in the

722   circum North Atlantic Basin, Journal of Nannoplankton Research. 37, 145–175, 2017.

723   Bolli, H.M., Saunders, J.B., and Perch-Nielsen, K.: Plankton Stratigraphy: Volume 1, Planktic

724   Foraminifera, Calcareous Nannofossils and Calpionellids. Cambridge University Press, 599 pp.,

725   1989.Boscolo-Galazzo, F., Crichton, K.A., Ridgwell, A., Mawbey, E.M., Wade, B.S., and Pearson

726   P.N.: Temperature controls carbon cycling and biological evolution in the ocean twilight zone,

727   Science, 371, 1148–1152, 2021.

728   Bown, P.R., and Young, J.R, Techniques. In: P.R. Bown (Ed.). Calcareous Nannofossil

729   Biostratigraphy, British Micropalaeontological Society Publications Series/Kluwer Academic,

730   London, 16–28 pp., 1998.

731   Bown, P.R., Lees, J.A., and Young, J.R.: Calcareous nannoplankton evolution and diversity

732   through time. In: H.R. Thierstein and J.R. Young (Editors), Coccolithophores: From Molecular

733   Processes to Global Impact. Springer, Berlin, 481-508, 2004.

734   Brombacher, A., Wilson, P.A., Bailey, I., and Ezard, T.H.: The Dynamics of Diachronous

735   Extinction Associated with Climatic Deterioration near the Neogene/Quaternary Boundary,

736   Paleoceanography and Paleoclimatology, e2020PA004205, 2021.

737   Browning, E., de Kaenel, E., Bergen, J.A., Blair, S.A., and Boesiger, T.M.: Oligocene-Pliocene

738   taxonomy and stratigraphy of the genus *Sphenolithus* in the circum North Atlantic Basin: Gulf of

739   Mexico and ODP Leg 154, Journal of Nannoplankton Research, 37, 77–112, 2017.

740 Ciummelli, M., Raffi, I., and Backman, J.: Biostratigraphy and evolution of Miocene Discoaster

741 spp. from IODP Site U1338 in the equatorial Pacific Ocean, J. Micropalaeontology, 36,

742 jmpaleo2015-034, 2016.

743 Coxall, H.K., Wilson, P.A., Pearson, P.N., and Sexton, P.F.: Iterative evolution of digitate

744 planktonic foraminifera. Paleobiology, 33, 495–516, 2007.

745 Cramer, B.S., Miller, K.G., Barrett P.J., and Wright, J.D.: Late Cretaceous–Neogene trends in deep

746 ocean temperature and continental ice volume: Reconciling records of benthic foraminiferal

747 geochemistry (d18O and Mg/Ca) with sea level history. J. Geophys. Res., 116, C12023, 2011.

748 Crichton K.A., Ridgwell A., Lunt D.J., Farnsworth A., and Pearson P.N.: Data-constrained

749 assessment of ocean circulation changes since the middle Miocene in an Earth system model. Clim.

750 Past https://doi.org/10.5194/cp-2019-151, 2020.

751 Crichton, K.A., Wilson, J.D., Ridgwell, A., and Pearson P.N.: Calibration of key temperature-

752 dependent ocean microbial processes in the cgenie.muffin Earth system model, Geosciences

753 Model Development, 14, 125–149, 2021.

754 Darling, K.F., Christopher, M.W., Stewart, I.A., Kroon, D., Dinglek, R. and Leigh Brown A.J.,

755 Molecular evidence for genetic mixing of Arctic and Antarctic subpolar populations of planktonic

756 foraminifers, Nature, 405, 43-47, 2000.

757 De Kaenel, E., Bergen, J.A., Browning, E., Blair, S.A., and Boesiger, T.M.: Uppermost Oligocene

758 to Middle Miocene Discoaster and Catinaster taxonomy and stratigraphy in the circum North

759 Atlantic Basin: Gulf of Mexico and ODP Leg 154, Journal of Nannoplankton Research, 37, 77–

760 112, 2017.

761 De Vargas, Renaud, C.S., Hilbrecht, H., and Pawlowski, J.: Pleistocene adaptive radiation in

762 Globorotalia truncatulinoides: genetic, morphologic, and environmental evidence, Paleobiology,

763 27, 104–125, 2001.

764 Davis, C.V., Wishner, K., Renema, W., and Hull, P.M.,: Vertical distribution of planktic

765 foraminifera through an oxygen minimum zone: how assemblages and test morphology reflect

766 oxygen concentrations, Biogeosciences, 18, 977–992, 2021.

767 Dowsett, H.J.: Diachrony of late Neogene microfossils in the Southwest Pacific Ocean: application

768 of the graphic correlation method, Paleoceanography, 3, 209-222, 1988.

769 Ezard, T.H.G., Aze, T., Pearson, P.N., and Purvis, A.: Interplay Between Changing Climate and

770 Species' Ecology Drives Macroevolutionary Dynamics, Science, 332, 349-351, 2011.

771 Fox, L.R., and Wade, B.S.: Systematic taxonomy of early–middle Miocene planktonic

772 foraminifera from the equatorial Pacific Ocean: Integrated Ocean Drilling Program, Site U1338,

773 The Journal of Foraminiferal Research 43, 374-405, 2013.

774 Fraass, A.J., Kelly, D.C., and Peters, S.E.: Macroevolutionary History of the Planktic

775 Foraminifera, Annu. Rev. Earth Planet. Sci., 431, 39–66, 2015.

776 Godrijan, J., Drapeau, D., and Balch, W.M.: Mixotrophic uptake of organic compounds by

777 coccolithophores, Limnology and Oceanography 00, 1–12, 2020.

778 Gibbs, S.J., Bown, P.R., Ward, B.A., Alvarez, S.A., Kim, H., Archontikis, O.A., Sauterey, B.,

779 Poulton, A.J., Wilson, J., and Ridgwell, A.: Algal plankton turn to hunting to survive and recover

780 from end-Cretaceous impact darkness, Sci. Adv. 6, eabc9123, 2020.

781   Greco, M., Jonkers, L., Kretschmer, K., Bijma, J., and Kucera, M.: Depth habitat of the planktonic

782   foraminifera Neogloboquadrina pachyderma in the northern high latitudes explained by sea-ice

783   and chlorophyll concentrations, Biogeosciences, 16, 3425–3437, 2019.

784   Hammer, Ø., Harper, D.A.T., and Ryan, P.D.: PAST: Paleontological Statistics Software Package

785   for Education and Data Analysis, Palaeontologia Electronica 4, 9 pp., 2001.

786   Henderiks, J., Bartol, M., Pige, N., Karatsolis, B.-T., and Lougheed, B.C.: Shifts in phytoplankton

787   composition and stepwise climate change during the middle Miocene, Paleoceanography and

788   Paleoclimatology, 35, e2020PA003915, 2020.

789   Herbert, T.D., Lawrence, K.T., Tzanova, A., Peterson, L.C., Caballero-Gill, R., and Kelly, C.S.:

790   Late Miocene global cooling and the rise of modern ecosystems. Nature Geoscience, 9, 843–847,

791   2016.

792   Hodell, D.A. and Vayavananda, A.: Middle Miocene paleoceanography of the western equatorial

793   Pacific (DSDP Site 289) and the evolution of Globorotalia (Fohsella), Marine Micropaleontology,

794   22, 279–310, 1993.

795   Hull P.M., and Norris R.D.: Evidence for abrupt speciation in a classic case of gradual evolution,

796   PNAS, 106, 21224–21229, 2009.

797   Hull, P. M., Osborn, K. J., Norris, R. D., and Robison, B. H.: Seasonality and depth distribution

798   of a mesopelagic foraminifer, Hastigerinella digitata, Monterey Bay, California, Limnol.

799   Oceanogr., 56, 562–576, 2011.

800   Itou, M., Ono, T., Olba, T., and Noriki, S.: Isotopic composition and morphology of living

801   Globoborotalia scitula: a new proxy of sub-intermediate ocean carbonate chemistry? Marine

802   Micropaleontology, 42, 189-210, 2001.

803   Jenkins, D.G. and Srinivasan, M.S.: Cenozoic planktonic foraminifers from the equator to the sub-

804   antarctic of the southwest Pacific, In: Kennett, J.P., von der Borch, C.C., Baker, P.A., Barton, C.E.,

805   Boersma, A., Caulet, J.P., et al., (Eds), Initial Reports of the Deep Sea Drilling Project 90, 795–

806   834, 1986.

807   John, E.H., P.N. Pearson, H.K. Coxall, H. Birch, B.S. Wade, and Foster G.L.: Warm ocean

808   processes and carbon cycling in the Eocene, Philos. Trans. R. Soc. A, doi:10.1098/rsta.2013.0099,

809   2013.

810   Jones, A.P., Dunkley Jones, T., Coxall, H., Pearson, P.N., Nala, D. and Hoggett, H.: Low-latitude

811   calcareous nannofossil response in the Indo-Pacific Warm Pool across the Eocene–Oligocene

812   Transition of Java, Indonesia. Paleoceanography and Paleoclimatology, 34, 1–15, 2019

813   Jonkers, L., and Kucera, M.: Global analysis of seasonality in the shell flux of extant planktonic

814   Foraminifera, Biogeosciences, 12, 2207–2226, 2015.

815   Kennett, J.P., and Srinivasan, M.S.: Neogene Planktonic Foraminifera. Hutchinson Ross

816   Publishing Co., Stroudsburg, Pennsylvania, 1-265 pp, 1983.

817   Kennett, J.P., and Von der Borch, C.C.: Southwest Pacific Cenozoic Paleoceanography. In

818   Kennett, J.P., von der Borch, C.C., et al., Initial Reports of the Deep Sea Drilling Project, 90:

819   Washington, DC (U.S. Government Printing Office), 1493–1517, 1986.

820   Kennett, J.P., and Exon, N.F.: Palaeoceanographic Evolution of the Tasmanian Seaway and its

821   Climatic Implications, In: Exon, N.F., Kennett, J.P., and Malone, M.J. (Eds.), The Cenozoic

822   Southern Ocean: Tectonics, Sedimentation, and Climate Change between Australia and

823   Antarctica. Geophysical Monograph, 151, 345–367, 2004.

824   Kim S.-T., and O'Neil J.R.: Equilibrium and non-equilibrium oxygen isotope effects in synthetic

825   carbonates. Geochim. Cosmochim. Acta, 61, 3461–3475, 1997.

826   Kucera, M., and Schonfeld, J.: The origin of modern oceanic foraminiferal faunas and Neogene

827   climate change, in Williams, M., Haywood, A.M., Gregory, F.J. and Schmidt, D.N. (eds) Deep-

828   Time Perspectives on Climate Change: Marrying the Signal from Computer Models and Biological

829   Proxies. The Micropalaeontological Society, Special Publications, The Geological Society,

830   London, 409–425, 2007.

831   Lam A.R., and Leckie R.M.: Late Neogene and Quaternary diversity and taxonomy of subtropical

832   to temperate planktic foraminifera across the Kuroshio Current Extension, northwest Pacific

833   Ocean, Micropaleontology, 66, 177–268, 2020a.

834   Lam, A. R., and Leckie, R. M.: Subtropical to temperate late Neogene to Quaternary planktic

835   foraminiferal biostratigraphy across the Kuroshio Current Extension, Shatsky Rise, northwest

836   Pacific Ocean, PLoS ONE, 15, e0234351, 2020b.

837   Lazarus, D.B., Hilbrecht, H., Spencer-Cervato, C. and Thierstein, H.: Sympatric speciation and

838   phyletic change in Globorotalia truncatulinoides, Paleobiology, 21, 28–51, 1995.

839 Lowery, C.M., Bown, P.R., Fraass, A.J. and Hull, P.M.,: Ecological Response of Plankton to

840 Environmental Change: Thresholds for Extinction, Annual Review of Earth and Planetary

841 Sciences, 48, 403-429, 2020.

842 Matsui, H., Nishi, H., Takashima, R., Kuroyanagi, A., Ikehara, M., Takayanagi, H., and Iryu, Y.:

843 Changes in the depth habitat of the Oligocene planktic foraminifera (Dentoglobigerina

844 venezuelana) induced by thermocline deepening in the eastern equatorial Pacific,

845 Paleoceanography, 31, 715-731, 2016.

846 Majewski, W.: Planktonic Foraminiferal Response to Middle Miocene Cooling in the Southern

847 Ocean (ODP Site 747, Kerguelen Plateau), Acta Palaeontologica Polonica, 55, 541-560,

848 2010.Meilland, J., Siccha, M., Weinkauf, M. F. G., Jonkers, L., Morard, R., Baranowski, U.,

849 Baumeister, A., Bertlich, J., Brummer, G. J., Debray, P., Fritz-Endres, T., Groeneveld, J., Magerl,

850 L., Munz, P., Rillo, M. C., Schmidt, C., Takagi, H., Theara, G., and Kucera, M.: Highly replicated

851 sampling reveals no diurnal vertical migration but stable species-specific vertical habitats in

852 planktonic foraminifera, J. Plank. Res., 41, 127–141, 2019.

853 Morard, R., Quillevere, F., Douady, C.J., De Vargas, C., De Garidel-Thoron, T., and Escarguel,

854 G.: Worldwide Genotyping in the Planktonic Foraminifer Globoconella inflata: Implications for

855 Life History and Paleoceanography, PLoS ONE 6(10): e26665, 2011.

856 Norris, R., D.: Pelagic Species Diversity, Biogeography, and Evolution, Paleobiology, 26, 236-

857 258, 2000.

858 Norris, R.D., and Corfield, R.M.: Evolutionary ecology of Globorotalia (Globoconella) (planktic

859 foraminifera), Marine Micropaleontology, 23, 121–145, 1994.

860   Norris, R.D. and de Vargas, C.: Evolution all at sea, Nature, 405, 23-24, 2000.

861   Norris, R.D., Corfield, R.M. and Cartlidge, J.E.: Evolution of depth ecology in the planktic

862   foraminifera lineage Globorotalia (Fohsella). Geology, 21, 975–978, 1993.

863   Norris, R. D., Kirtland Turner, S., Hull, P. M., and Ridgwell, A.: Marine Ecosystem Responses to

864   Cenozoic Global Change, Science, 341, 492-498, 2013.Pearson, P.N.: Planktonic foraminifer

865   biostratigraphy and the development of pelagic caps on guyots in the marshall islands group, In:

866   Haggerty, J.A., Premoli Silva, I., Rack, R., and McNutt, M.K. (Eds.), Proceedings of the Ocean

867   Drilling Program, Scientific Results, 144, 21-59, 1995.

868   Pearson, P.N., and Coxall, K.H.: Origin of the Eocene planktonic foraminifer Hantkenina by

869   gradual evolution, Palaeontology 57, 243–267, 2012.

870   Pearson, P.N., N.J. Shackleton, and Hall M.A.: Stable isotopic evidence for the sympatric

871   divergence of Globigerinoides trilobus and Orbulina uniriersa (planktonic foraminifera), Journal

872   of the Geological Society, 154, 295-302, 1997.

873   Quillevere F., Norris R.D., Moussa I., and Berggren W.A.: Role of photosymbiosis and

874   biogeography in the diversification of early Paleogene acarininids (planktonic foraminifera),

875   Paleobiology, 27, 311–326, 2001.

876   Quinn, P.S., Cortés, M.Y. and Bollmann, J.: Morphological variation in the deep ocean-dwelling

877   coccolithophore Florisphaera profunda (Haptophyta), European Journal of Phycology, 40, 123-

878   133, 2005.

879   Raffi, I., Wade, B.S., Pälike, H., Beu, A.G., Cooper, R., Crundwell, M.P., Krijgsman, W., Moore,

880   T., Raine, I., Sardella, R., and Vernyhorova, Y.V.: Chapter 29 - The Neogene Period, Editor(s):

881   Felix M. Gradstein, James G. Ogg, Mark D. Schmitz, Gabi M. Ogg, Geologic Time Scale 2020,

882   Elsevier, 1141-1215 pp., 2020

883   Rebotim, A., Voelker, A. H. L., Jonkers, L., Waniek, J. J., Meggers, H., Schiebel, R., Fraile, I.,

884   Schulz, M., and Kucera, M.: Factors controlling the depth habitat of planktonic foraminifera in the

885   subtropical eastern North Atlantic, Biogeosciences, 14, 827–859, 2017.

886   Schiebel, R., and Hemleben, C.: Planktic Foraminifers in the Modern Ocean, Springer-Verlag,

887   Berlin Heidelberg, 2017.

888   Schiebel R., Smart S.M., Jentzen A., Jonkers L., Morard R., Meilland J., Michel E., Coxall H.K.,

889   Hull P.M., De Garidel-Thoron T., Aze T., Quillévéré F., Ren H., Sigman D.M., Vonhof H.B.,

890   Martínez-García A., Kucera M., Bijma J., Spero H.J., and Haug G.H., Advances in planktonic

891   foraminifer research: New perspectives for paleoceanography, Revue de micropaléontologie, 61,

892   113–138, 2018.

893   Schneider, C., and Kennett, J.: Isotopic evidence for interspecies habitat differences during

894   evolution of the Neogene planktonic foraminiferal clade Globoconella, Paleobiology, 22, 282-303,

895   1996.

896   Schneider, C., and Kennett, J.: Segregation and speciation in the Neogene planktonic foraminiferal

897   clade Globoconella, Paleobiology, 25, 383-395, 1999.

898 Scott, G.H., Bishop, S., and Burt, B.J.: Guide to some Neogene Globorotalids (Foraminiferida)

899 from New Zealand. New Zealand Geological Survey Paleontological Bulletin 61, Lower Hutt,

900 New Zealand, 176 pp., 1986.

901 Scott, G.H., Bishop, S., and Burt, B.J.: Guide to some Neogene Globorotalids (Foraminiferida)

902 from New Zealand. New Zealand Geological Survey Paleontological Bulletin 61, Lower Hutt,

903 New Zealand, 176 pp., 1990.

904 Sosdian, S.M., Greenop, R., Hain, M.P., Foster, G.L., Pearson, P.N., and Lear, C.H.: Constraining

905 the evolution of Neogene ocean carbonate chemistry using the boron isotope pH proxy, Earth and

906 Planetary Science Letters, 498, 362–376, 2018.

907 Spezzaferri, S., Kucera, M., Pearson, P.N., Wade, B.S., Rappo, S., Poole, C.R., Morard, R.,

908 Stalder, C.: Fossil and genetic evidence for the polyphyletic nature of the planktonic foraminifera"

909 Globigerinoides", and description of the new genus Trilobatus, PLoS One 10, e0128108, 2015.

910 Stainbank, S., Kroon, D., Ruggeberg, A., Raddatz, J., de Leau, E.S., Zhang, M., and Spezzaferri,

911 S.: Controls on planktonic foraminifera apparent calcification depths for the northern equatorial

912 Indian Ocean, PLoS ONE, 14, e0222299, 2019.

913 Styzen, M.J.. Cascading counts of nannofossil abundance, Journal of Nannoplankton Research,

914 19, 49, 1997.

915 Super, J.R., Thomas, E., Pagani, M., Huber, M., O'Brien, C.L., and Hull, P. M.: Miocene evolution

916 of North Atlantic Sea surface temperature. Paleoceanography and Paleoclimatology, 35,

917 e2019PA003748, 2020.

918   Wade, B.S., Pearson, P.N. Berggren, W.A. and Palike, H.: Review and revision of Cenozoic

919   tropical planktonic foraminiferal biostratigraphy and calibration to the geomagnetic polarity and

920   astronomical time scale, Earth-Science Reviews, 104, 111–142, 2011.

921   Wade, B.S., Pearson, P.N., Olsson, R.K., Fraass, A. Leckie, R.M. and Hemleben, Ch.: Taxonomy,

922   biostratigraphy, and phylogeny of Oligocene and lower Miocene Dentoglobigerina and

923   Globoquadrina, in Wade, B.S., Olsson, R.K., Pearson, P.N., Huber, B.T. and Berggren, W.A.,

924   Atlas of Oligocene Planktonic Foraminifera, Cushman Foundation of Foraminiferal Research,

925   Special Publication, No. 46, p. 331-384, 2018.

926   Wei, K.Y.: Stratophenetic tracing of phylogeny using SIMCA pattern recognition technique: A

927   case study of the late Neogene planktic foraminifera Globoconella clade, Paleobiology, 20, 52-65,

928   1994.

929   Wei, K.Y., and Kennett, J.P.: Taxonomic evolution of Neogene planktonic foraminifera and

930   paleoceanographic relations, Paleoceanography, 1, 67-84, 1986.

931   Wei, K.Y., and Kennett, J.: Phyletic gradualism and punctuated equilibrium in the late Neogene

932   planktonic foraminiferal clade Globoconella, Paleobiology, 14, 345-363, 1988.

933   Weiner, A., Aurahs, R., Kurasawa, A., Kitazato, H., and Kucera, M.: Vertical niche partitioning

934   between cryptic sibling species of a cosmopolitan marine planktonic protest, Mol. Ecol., 21, 4063–

935   4073, 2012.

936   Woodhouse, A., Jackson, S.L., Jamieson, R.A., Newton, R.J., Sexton, P.F., and Aze, T.: Adaptive

937   ecological niche migration does not negate extinction susceptibility. Scientific Reports, 11, 15411,

938   2021.

939   Young, J.R., Bergen, J.A., Bown, P.R., Burnett, J.A., Fiorentino, A., Jordan, R.W., Kleijne, A.,

940   van Niel, B.E., Romein, A.J.T. and Von Salis, K.: Guidelines for coccolith and calcareous

941   nannofossil terminology, Palaeontology, 40, 875–912, 1997.

942   Zhang, Y.G., Pagani, M., Liu Z.: A 12-Million-Year Temperature History of the Tropical Pacific

943   Ocean, Science, 344, 84-87, 2014.

944   Zenodo DOI: 10.5281/zenodo.4469673.

945   Zenodo DOI: 10.5281/zenodo.4469678.